Lawrence Berkeley National Laboratory
Lawrence Berkeley National Laboratory

Title
INVESTIGATION OF WEAR RESISTANT MATERIAL USING DISPERSED PHASE INTERMETALLIC COMPOUND OF NICKEL-TITANIUM-SILICON IN AN IRON MATRIX

Permalink
https://escholarship.org/uc/item/7pq5h5vg

Author
Steinmetz, C.

Publication Date
1977-12-01

eScholarship.org Powered by the California Digital Library
University of California

LBL-6983
c.2

INVESTIGATION OF WEAR RESISTANT MATERIAL USING DISPERSED PHASE INTERMETALLIC COMPOUND OF NICKEL-TITANIUM-SILICON IN AN IRON MATRIX

Charles Steinmetz
(M. S. thesis)

RECEIVED
LAWRENCE
BERKELEY LABORATORY
MAY 31 1978
LIBRARY AND
DOCUMENTS SECTION

December 1977

Prepared for the U. S. Department of Energy
under Contract W-7405-ENG-48

TWO-WEEK LOAN COPY

This is a Library Circulating Copy which may be borrowed for two weeks. For a personal retention copy, call Tech. Info. Division, Ext. 6782

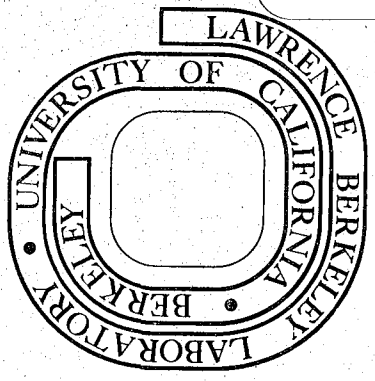

LBL-6983
C.2

DISCLAIMER

This document was prepared as an account of work sponsored by the United States Government. Neither the United States Government nor any agency thereof, nor The Regents of the University of California, nor any of their employees, makes any warranty, express or implied, or assumes any legal liability or responsibility for the accuracy, completeness, or usefulness of any information, apparatus, product, or process disclosed, or represents that its use would not infringe privately owned rights. Reference herein to any specific commercial product, process, or service by its trade name, trademark, manufacturer, or otherwise, does not necessarily constitute or imply its endorsement, recommendation, or favoring by the United States Government or any agency thereof, or The Regents of the University of California. The views and opinions of authors expressed herein do not necessarily state or reflect those of the United States Government or any agency thereof or The Regents of the University of California and shall not be used for advertising or product endorsement purposes.

Lawrence Berkeley Laboratory is an equal opportunity employer.

INVESTIGATION OF WEAR RESISTANT MATERIAL USING DISPERSED PHASE INTERMETALLIC COMPOUND OF NICKEL-TITANIUM-SILICON IN AN IRON MATRIX

by

Charles Steinmetz

Materials and Molecular Research Division,
Lawrence Berkeley Laboratory and
Department of Mechanical Engineering
University, of California, Berkeley, CA 94720

INVESTIGATION OF WEAR RESISTANT MATERIAL USING DISPERSED PHASE INTERMETALLIC COMPOUND OF NICKEL-TITANIUM-SILICON IN AN IRON MATRIX

Contents

Abstract. vi

I. Introduction 1

II. Wear Mechanisms. 4

III. Materials and Experimental Methods

- A. Powder Characteristics. 7
- B. Blending and Compacting 8
- C. Sintering 9
- D. Density Measurement 9
- E. Metallography 9

IV. Friction and Wear Test Machine

- A. Test Apparatus. 11
- B. Instrumentation 11

V. Wear Test Approach

- A. Test Procedure and Conditions 14
- B. Basis for Test Conditions 14

VI. Results and Discussion

- A. Sintering Process 16
- B. Particle and Matrix Interaction 16
- C. Densification 18
- D. Friction and Wear Tests 19

VII. Conclusions and Recommendations

- A. Conclusions 23
- B. Recommendations 24

Acknowledgment. 25

Appendix 26

References 29

Tables: I through IV 32

Figure Captions 37

Figures 39

INVESTIGATION OF WEAR RESISTANT MATERIAL USING DISPERSED PHASE INTERMETALLIC COMPOUND OF NICKEL-TITANIUM-SILICON IN AN IRON MATRIX

by

Charles Steinmetz

Materials and Molecular Research Division,
Lawrence Berkeley Laboratory and
Department of Mechanincal Engineering
University, of California, Berkeley, CA 94720

ABSTRACT

The physical and mechanical properties of iron powder blended with a hard intermetallic compound, Ni_3Ti_2Si, were studied in the as-sintered condition.

The influence of the morphology on the wear tests was investigated using a pin-on-disk wear test machine. The variables affecting the morphology of this system have been experimentally determined.

1. INTRODUCTION

The need to control the wear of materials is important now more than ever before because of the importance of greater conservation in energy and materials. With the advent of new energy systems, such as coal liquefaction and gasification, there is a need for materials that will withstand their extreme operating conditions. These materials need to function at high temperatures, in corrosive and erosive environments.

The study of wear was initially restricted to minimizing friction by lubricants. Today this constitutes only part of the field of research, referred to as tribology.[1]

During the forties and fifties, increasing interest was devoted to the microevents during wear. Theoretical models were developed for the wear of surfaces under relative sliding. Some of these models still form the basis of current theories and are summarized in a standard work by Bowden and Tabor.[2] In the 1960's the emphasis of wear research was on experimental verifications of suggested hypotheses.

Materials such as cemented carbides and dispersed oxides have been used in wear resistant applications for years. Cemented carbides, dispersed oxides and superalloys have been tried and tend to wear excessively in the new energy systems.[3]

Cemented carbides and dispersed oxides are products of powder metallurgy. They consist of hard particles in a softer binder matrix. For tungsten-carbide-cobalt, the maximum operating temperature is 540°C; the limitation is the cobalt matrix. For Steel-Bonded Titanium Carbide, the maximum operating temperature is 420°C. At this temperature

the steel matrix softens rapidly. Dispersed oxides are also limited by the temperature effects on the matrix.[4]

With carbides and oxides, there is no metallurgical bond with the surrounding matrix. Without this bond these particles tend to dislodge from the matrix and act as abrasive particles. These particles can be dislodged by softening or structural change of the matrix at high temperatures, by the matrix around the particles being worn away, or by cyclic stresses on the surface thereby loosening the particles in the matrix.[5]

Another addition to the list of wear resistant materials in recent years, is the use of hard intermetallic compounds. The commercially available, hard intermetallic compounds can be dispersed in various matrices, giving a variety of properties. Intermetallic compounds have the advantage of being able to metallurgically bond to compatible matrices, therefore improving the composite's wear properties.

At a hardness of approximately 1100 VHN (Vickers Hardness Number), the intermetallic dispersed phase is softer than the common wear-resistant additives of carbides and oxides, of approximately 2000 VHN. Therefore, under selective operating conditions the carbides and oxides would perform better than hard intermetallics.

The first stage of the investigation involved the selection of materials with desirable characteristics, to be adaptable to a wide range of service requirements. The materials selected were in the ternary Nickel-Titanium-Silicon system and they provide hard phases with desirable properties to be dispersed in appropriate metallic matrices. This alloy system contains several ternary intermetallic

compounds, of which the G, G', V, E and F phases all have desirable properties.[6]

For this investigation, the compound studied was the G' Laves phase with a composition corresponding to Ni_3Ti_2Si. This compound was selected because:

1. It is a hard phase - 1000 Vickers hardness.
2. The component elements impart good corrosion resistance.
3. It has good high temperature stability.
4. It interacts with selected matrices, to form a broad diffusion layer, thus providing good metallurgical bonding.

For this investigation, the composites consisted of G' particles dispersed in an iron matrix. This matrix was chosen for the initial study because friction and wear studies of sintered iron, and composites of the commercial intermetallic additive dispersed in an iron matrix, have been previously documented.[7,8,9,10] This commercial product has the same structure as the G' phase, and became the standard, against which the new material was judged.

The composition studied was iron plus 20% by weight G' phase. The influence of the morphology on the wear resistance of this composite was observed. The variables used in controlling the morphology of the G' phase dispersed in the iron matrix were the sintering time and temperature.

To measure the wear rates of this material, a wear test machine was required. The first part of this project involved the design and construction of a pin-on-disk friction and wear test machine.

II. WEAR MECHANISMS

Wear can be defined as the progessive loss of substance resulting from mechanical interaction between two contacting surfaces. In general, these surfaces will be in relative motion, either sliding or rolling, and under load. Wear occurs because of the local mechanical failure of highly stressed interfacial zones, and the failure mode often will be influenced by environmental factors. Surface deterioration can lead to the production of wear particles by a series of events, characterised by adhesion and particle transfer mechanisms; or by a process of direct particle production: similar to machining; or a surface fatigue form of failure; or by chemical reaction with the surface. The four mechanisms are referred to as adhesive, abrasive, fatigue and corrosive wear, and are the four most important.

The terms cohesion and adhesion, refer to the ability of atomic structures to hold themselves together and form surface bonds with other atoms or surfaces with which they are in contact. Two clean surfaces of similar crystal structure will adhere strongly to one another simply by placing them in contact. In practice, this generally does not occur because of surface contamination. Measurable adhesion is only shown when the surfaces are loaded and translated with respect to each other, causing the surface films to break up. Plastic deformation frequently occurs at the contacting areas under high loading; this greatly assists with the disruption of the oxide films.[11]

The actual establishment of a bond is only the first stage of this wear mechanism. The bonded region may be strengthened by work

hardening; shear may occur within the body of one of the two surfaces, thus allowing a fragment of material to be transferred from one surface to another.[12] See Figure 1 for a simplified picture of adhesive wear.

Quantitative laws for adhesive wear have been developed, and are used by designers to predict adhesive wear rates.[13] The simplest and oldest adhesion model for wear was advanced by Archard.[14]

Abrasive wear can be caused either by hard abrasive particles entrapped between two sliding surfaces, or by the asperities of a hard surface sliding on a soft surface. The mechanism of abrasive wear consists of material removal, by cutting of the surface by hard loose particles or asperties on the mating surface as shown in Figure 2.

The abrasive wear volume is, to a first approximation, proportional to the normal load and the distance slid, and inversely proportional to the hardness. This approximation was developed by Rabinowicz.[15] Many wear processes change into abrasive wear when loose wear particles are generated.

The fatigue wear mechanism can operate under sliding wear conditions; they tend to occur more predominantly in rolling contact where the stresses are high and slip is small. The fatigue wear mechanism gives rise to pitting or spalling of bearing surfaces.[16] The mechanism is closely related to the failure mechanism of fracture and fatigue in bulk materials. Stress in the material builds up as a result of the contact stresses until the material suddenly fractures, starting from an initiating crack near the surface; a sizeable wear fragment is formed as a result of this process.

Corrosion wear is not a material removal process: that is in the same sense as adhesion, abrasion, and fatigue are, because corrosion is the degradation of a surface by chemical means.

Many wear processes start with adhesive and fatigue mechanisms, but the fact that wear processes lead to the generation of debris, inevitably means that there is always a possibility that it may change to one of abrasion. The corrosion mechanism may enhance the other mechanisms during the wear process.

III. MATERIALS AND EXPERIMENTAL METHODS

A. Powder Characteristics

Characteristic of the elemental iron powder used in this study, are shown as manufacturer's data in the following table. The characteristics of the commercial intermetallic compound used in some specimens are shown in Table 1, page 32.

	Fe*
Chemical Analysis - Cu	0.0
C	0.01
S	0.01
P	0.005
Mn	0.2
Si	0.02
Fe	Balance
H_2 loss	0.12
Screen analysis	%
-80 + 100	2.0
-100 + 150	14.0
-150 + 200	22.0
-200 + 250	10.0
-250 + 325	22.0
-325.	30.0
Apparent Density	2.95 g/cm^3
Flow time	25 sec/50g

*EMP atomized, grade 300 m, Lot #1455, A. O. Smith Company

The Nickel - Titanium - Silicon alloy was cast into an ingot, which was crushed and then ball-milled in hexane to a mesh size of -400. An x-ray examination showed the alloy to be an intermetallic compound wih a structure of Ni_3Ti_2Si: the G' phase of this ternary system. The composition of this phase, in atomic percent, is 58.70% Nickel, 31.90% Titanium, and 9.36% Silicon. The measured density was 5.71 g/cm^3. The compound had a silvery luster and was very brittle.

B. Blending and Compacting

The powders were weighed to the desired composition, and then tumble blended together with alumina pellets for 24 hours. The alumina pellets sufficiently broke up agglomerated powders and aided in producing a uniform powder mixture. After blending, the mixture of powders was pressed in a single acting steel die, using a hydraulic press to obtain the desired specimen shape. The powders were compacted to a pressure of 6.90×10^8 Nt/m^2 (100,000 psi), and held under pressure for over one minute to allow for outgassing. All die surfaces were lubricated before each compacting process. The lubricant used was a mixture of 100 gm. of zinc stearate in one liter of methylchloroform (1.1.1 - trichloroethane). After the die-compacting process, the compacts were then isostatically pressed to a pressure of 6.9×10^8 Nt/m^2. The second compacting process was done to obtain a more uniform green density. For the isostatic compaction, the specimens were sealed in a flexible container and held under pressure for over one minute.

C. Sintering

All samples, after the compacting processes, were sintered in a vacuum furnace (Brew Company). The samples were sintered in aluminum oxide crucibles and were set at the middle of the furnace hot zone.

A platinum - rhodium "Type S" thermocouple was used to measure the sintering temperature. This thermocouple was also set at the middle of the furnace hot zone in the crucible containing the sample, but not in direct contact with it.

D. Density Measurement

All of the samples had their density measured by a volume displacement method. Before immersing the samples in the distilled water, they were first vacuum impregnated with epoxy resin, which filled up the pores to prevent the penetration of water into the samples.

During immersion, the samples were held in a wire cage with the cage suspended by a thin wire. The interaction of surface tension between the suspension wire and the water's surface, influenced the weight measurment of the immersed samples. To reduce this surface tension, a few drops of Kodak 200 Photo flow solution were added to 100 ml of distilled water.[17]

E. Metallography

All samples prepared for metallographic examination mounted in Bakelite. After the samples were mounted, they were abraded on silicon carbide papers down to 325 grit; then abraded on emery paper to 4/0, and at that time carefully polished

on a 1 μ diamond wheel. They were then finally micropolished with 0.05 micron, Leco Finish-Pol, to remove any pieces of diamond impregnated in the surface.

This technique gave satisfactory resolution of the polished surface at 1000X under the optical microscope. Before examination, the samples were etched with a solution of one part Marble's solution to twenty parts distilled water. With this solution, the etching time was usually about 10 - 20 seconds, depending on the sample.

Scanning electron microscopy (SEM) and EDAX (Energy Dispersive Analysis of X-Rays) were used to distinguish the phases present.

IV. FRICTION AND WEAR TEST MACHINE

A. Test Apparatus:

The friction and wear test machine designed and constructed at the Materials and Molecular Research Division, was of the pin-on-disk type.

The active components of the machine are a straight pin, being the test material of circular cross-section and flat at ends, sliding against a rotating disk. Figure 3 shows the pin and disk wear surfaces. The pin is supported parallel to the axis of the disk, with the aid of a holder. The holder is supported by the load arm, which can rotate in two directions around one point, using a gimbal system. This arrangement allows a load to be transmitted to the pin, and the frictional force to be transferred to a measuring device. At one end of the load arm is the counterbalance weight; this can be adjusted to balance the load arm with the specimen attached. At the other end of the load arm is mounted the applied weight. The friction force between the pin and disk is measured with the aid of strain gages mounted on a beam, which also prevents the load arm from swinging off of the disk during a test. Figure 4 shows the component parts to the test apparatus.

The pin-on-disk type of friction and wear test machine offers the most convenient way of controlling the important test parameters for a friction and wear test, namely:

1. sliding speed
2. normal force
3. sliding distance

The relative sliding speed between the pin and disk is controlled by the angular velocity of the disk, which is directly driven by an electric motor. The motor is a DC variable speed unit with a feedback speed control system, to compensate for fluctuating loads. With this motor, the test apparatus can run tests at various sliding speeds from 0.1 m/sec to 50 m/sec.

The normal force on the specimen is controlled by the mass of the applied weight mounted on the load arm. With the motor's torque and power rating, the machine can make tests of up to 18 kg load on the specimen. Since there is a counterbalance on the load arm, very small loads can be applied to the specimen accurately.

The sliding distance for a test can be controlled by selecting the duration of a test, at a specific sliding speed.

Several views of the friction and wear test machine are shown in Figures 5 through 7.

B. Instrumentation

To measure the sliding speed, frictional force, and specimen equilibrium temperature, various instruments were used. The sliding speed is a function of the motor rpm; the motor rpm is monitored by measuring the output from the tach-generator that is connected to the motor. To monitor the frictional force, the strain gage assembly is connected to a Tektronix Q-Plug unit

amplifier; the output is continuously recorded with the aid of a Clevite-Brush Mark 220 pen recorder. The specimen equilibrium temperature is measured by means of a thermocouple pressed into a hole in the pin, 2.5 mm from the wear surface, at the beginning of a test. These instruments, and the test machine, are shown in Figure 8. A schematic of the instrumentation is shown in Figure 9. The details of the test pin are shown in Figure 10.

V. WEAR TEST APPROACH

A. Test Procedure and Conditions

All tests were conducted in air, under unlubricated conditions. The pins (specimens) were ground to a surface finish of 1.00 micron center line average (c.l.a.) and were ultrasonically cleaned in acetone. The wear disk, against which the wear specimens were rubbed, was made of AISI 52100 bearing steel. The disks were hardened to a Rockwell "C" hardness of 55-60, depending on the particular disk used. The disks were ground to a surface finish of c.l.a. 0.405-0.611 microns, and then ultrasonically cleaned in acetone to remove any traces of lubricant.

The ambient temperature during the tests was 22-27^{o}C, with a relative humidity of 55 - 70%. The tests were conducted at a relative sliding speed of 2 ms^{-1}, and a contact pressure of 19.8 kgf cm^{-2}. The test durations were usually 2 hours in length.

The dimensions and weight of the specimen and disk were measured before, half-way, and after each test. Wherever possible, the standard procedures proposed at the international cooperative wear test program were followed.[18] For a step-by-step procedure of a test, see the Operation Manual in the Appendix.

B. Basis for Test Conditions

The basis for selecting the test conditions, namely the applied load and sliding speed, was that of using similar conditions from other wear studies of similar materials.[19,20] The applied load was higher than that used by others, but to emphasize the wear of the materials being studied, an excessive load was applied.

This excessive load also simulated extreme operating conditions for this type of material.

VI. RESULTS AND DISCUSSION

A. Sintering Process

For the composite of G' phase dispersed in an iron matrix, the desired microstructure would be the hard G' particles with a broad diffusion band around them, with these particles being dispersed evenly throughout the matrix. Along with these desired features, a density close to theoretical would be important.

It has been found that sintering time and sintering temperature are of great importance in the morphological control of the G' phase dispersed in the iron matrix. Not only are the effects of these two variables visible in obtaining the amount of diffusion between the particles and matrix, but also in the porosity of the final product. Both of these effects influence the wear properties of this material.

For the composition studied, three different sintering times and temperatures were tried. The sintering temperatures used were 1000°C, 1150°C, and 1250°C. The sintering times at these temperatures were 15, 30, and 60 minutes. Also a set of samples were studied that had been arc-melted in a vacuum arc-furnace and then homogenized at 1150°C, under vacuum, for one hour. See Table II for the sintering parameters used on the wear samples tested.

B. Particle and Matrix Interaction

The green compact (no sintering) of the material shown in Figure 11, shows fair distribution of the G' particles with the coarse iron particles.

By using a Leitz miniload hardness tester, with a 100 gram load, the hardnesses of the material were measured. After sintering, the pure EMP iron compacts had a hardness of 80VHN, which is typical for sintered iron. The G' phase has a much higher hardness of 1000 VHN.

The amount of interdiffusion between the G' particles and the iron matrix, increased wih sintering time and temperature. This interdiffusion results in the formation of the metallurgical bond between the hard particles and the matrix. The magnitude of the diffusion also causes a decrease in size of the G' particles and hardening of the iron matrix. The iron matrix was solution hardened by the nickel, titanium and silicon from the G' phase particles. In Figure 12, this interaction is shown with composition and hardness of each phase for the sintering temperatures of 1000°C and 1150°C. This figure also shows that at the sintering temperature of 1150°C, there is more complete bonding around the entire particle than at 1000°C. The effect is also displayed in Figures 13 and 14 at these sintering temperatures.

Compacts were also sintered at 1250°C for one hour and arc-melted. At these temperatures, the structure contained no more G' phase particles; there was almost complete diffusion of the elements. Figure 15 shows the structure after sintering at 1250°C for one hour. Notice that no discrete G' particles exist, but a fine eutectic looking structure is formed. For the arc-melted compact shown in Figure 16, the structure is similar to that shown in Figure 15. The compositions given by the EDAX x-ray

analyses, are also very similar. The microhardness of both of these materials was 490 VHN.

These structures, without the hard particles present, are undesirable because of their wear properties.

See Table III for the general hardness of all the samples tested.

C. Densification

For the composition studied in this project, the green densities were approximately 90% of the theoretical density. They were this high because of the double compacting process. The sintered densities varied with sintering time and temperature, and are shown in figure 17. See Table III for a list of densities of all the samples.

A swelling of the compacts occurred when sintered at 1150°C; this explains the reduction in density when sintering at this temperature. A small amount of liquid phase occurs at this temperature, and may have penetrated into the grain boundaries causing them to separate; thus resulting in increasing the volume of the specimens. An increase of 10% was measured in the dimensions after sintering at 1150°C. Figure 14, shows a series of specimens sintered at 1150°C for various times; these show good bonding around the G' phase particles.

For the compacts sintered at 1000°C, there was no swelling; in fact there was a slight reduction in dimensions. At this temperature, the sintered densities were a little higher than the green density, as shown in Figure 17. In figure 13, the

photomicrographs of this series may be misleading because they seem to show a large amount of porosity. These pores may have been locations of hard G' particles, but during the polishing process, they may have been pulled out.

The attainment of close to theoretical density in composite powder-metallurgy materials, is crucial in acquiring the maximum mechanical properties.[21]

The effect of porosity on the wear properties is two-fold; with small amounts it can be helpful, but too much porosity results in poor wear properties.

Experimental evidence has supported the concept that pores of small size, do not act as internal crack nucleation sites, but can do so for external free surfaces.[22] For higher porosity, the micromechanisms of fracture is related to the coalescence of pores.[23] This results in large material removal.

D. Friction and Wear Tests

Friction and wear tests were conducted on three different materials: sintered iron, iron plus 22 w/o* commercial additive, and iron plus 20 w/o G' phase. Table IV gives a summary of all the wear tests conducted in this investigation.

The friction and wear tests were conducted on sintered iron to compare the results with other studies, and to use as a comparison for other materials tested. The results compared favorably with other studies of sintered iron.[24,25]

* weight percent

The tests conducted on the iron plus the commercial additive, were also used as a comparison for the iron plus G' phase material. This material was sintered using the manufacturer's recommendations. Figure 18 shows a photomicrograph of the iron plus the additive. Tests conducted elsewhere on this material, were subject to different test conditions.[26]

For the iron plus G' phase, there were three series of tests made, all of which used different sintering processes. They were sintered at 1150°C, sintered at 1000°C, and arc-melted. For the samples sintered at 1150°C, the wear rate as a function of sintering time, is given in Figure 19. Figure 20 gives the coefficient of friction from the tests, as a function of the sintering time of the samples.

An immediate observation from the friction and wear tests, is that the coefficient of friction changes slightly while the wear rates varied by orders of magnitude.

This condition has been documented by other experimenters who state that for most metal combinations, the coefficient of friction is usually between 0.5 and 1.5, while the wear rates may vary by orders of magnitude.[27]

The wear rates for all the materials tested in this project, are graphically shown in Figure 21. For the series of iron plus G' phase sintered at 1150°C, there was an increase in the wear rate by orders of magnitude between the samples sintered for 30 minutes and 60 minutes. This was caused by the different wear mechanisms involved in each. The series of samples that were

arc-melted wore excessively fast like that of samples sintered at 1150°C for 60 minutes.

The type of wear debris collected during a wear test, gives a good indication of the wear mechanisms involved. An x-ray analysis of wear debris from one of the tests, showed a mixture of iron oxide and base material; the iron oxide was a dark gray to black in color, and was a fine powder. For all the tests conducted, except those samples of iron plus G' that were sintered at 1150°C for 60 minutes and those that were arc-melted, similar wear debris was observed.

Figure 22a, shows a wear pin after a wear test. The dark areas are a layer of iron oxide; Figure 22b shows some of the wear debris collected from this pin.

The wear debris collected during the tests of the samples that were sintered at 1150°C for 60 minutes and that were arc-melted were very similar. Their debris had a silvery luster, and were larger in size than the oxide debris.

Under metal to metal sliding conditions, the frictional heating of the surfaces causes oxides to form; the hard stable oxides form a wear-resistant layer. The formation of this hardened surface is instrumental in reducing wear rates of sintered metals.[28]

The wear mechanisms involved in all the tests are a combination of the four mechanisms discussed in an early section; the magnitudes of each mechanism may be different. Since this investigation was not an intensive study of the wear mechanisms

involved, only speculative conclusions on the wear mechanisms involved can be given. The wear mechanisms that took place on the samples that form oxide layers, may have been adhesive wear of the exposed pin material, and abrasive wear from the loosened oxides and pin material. This is similar to results obtained by Amsallem, Gaucher and Guilhot, on their study of sintered iron.[29]

The wear mechanisms that might have been involved for the samples that produced no oxides and wore excessively fast, are adhesive wear that produce the large particles, thus causing major abrasive wear.

In this investigation, the important results of the wear tests are that the Fe + 20 w/o G' material is more wear resistant than the Fe + 22 w/o commercial additive under these wear test conditions. Figure 21, shows how the wear rates of these two materials compare.

VII. CONCLUSIONS AND RECOMMENDATIONS

A. Conclusions

1. At a sintering temperature of 1150°C, a large amount of interdiffusion between the hard G' particles and iron matrix occurred. This interdiffusion produced softening of the particles and hardening of the matrix. Also at this sintering temperature, complete bonding around the entire particle occurred.
2. Swelling of the compacts is observed during sintering at 1150°C. Both diffusion and boundary penetration contributed to the swelling of the compacts.
3. At a sintering temperature of 1000°C, little interdiffusion occurred, but a small diffusion band around the hard particles was formed. This diffusion band was not distributed completely around the particles. With this limited interdiffusion, the G' particles remained much harder than the iron matrix.
4. The friction and wear results of sintered iron are consistent with other published data, as previously mentioned. This indicated the friction and wear test machine used is consistent with other existing friction and wear test machines.
5. The wear resistance of Fe + 20 w/o G' is greatly dependent on the thickness of the diffusion band around the hard particles. When the material was arc-melted and no discrete hard particles remained, it wore ex-

cessively fast. However, when the material was sintered at 1000°C and 1150°C, the hard particles, with some bonding to the matrix existing, provided much better wear resistance.

6. A definite improvement in wear resistance of sintered iron was observed when hard particles, either the commercial additive or the G' phase, were dispersed in the iron matrix. For the same friction and wear test conditions, the wear rate of Fe + 20 w/o G' was one-fifth that of the Fe + 22 w/o commercial additive. This gives a good indication that using the dispersed G' phase does have definite potential of being an excellent wear resistant material.

B. Recommendations

1. Further investigatons into the improvement of the wear resistance of the G' phase dispersed in an iron matrix, would include other sintering times, temperatures, and mixing processes. The sintering temperatures that should be tried next, are 1050°C and 1100°C at various sintering times. Possible changes in the mixing process could be to lengthen the tumble mixing duration. Another possibility for improving the wear resistance, would be the determination of the optimum amount of the hard phase compound.

2. A possible method to improve the microstructure, would be to use a diffusion retarder. This would slow the

diffusion process between the G' particles and the iron matrix, and thus permit longer sintering times to improve the densification and bonding. If a small percentage of the constituent elements from the G' phase, that is, nickel, titanium and silicon, were mixed in with the iron powder, then this would act as a diffusion retarder.

3. The possibilities of this hard phase being dispersed in other metallic matrices, such as high nickel alloys, should also be investigated. This investigation may lead to a material adaptable to other service conditions.

ACKNOWLEDGMENT

The author is sincerely grateful to Professor Milton R. Pickus for his advice and guidance. Special thanks to Dr. John Ling-Fai Wang for his encouragement and valuable directions throughout the project. The technical assistance rendered by Mr. John T. Holthuis and Mr. John A. Jacobsen and the machinists in the shop at M.M.R.D. is greatly appreciated.

This work was supported by the Division of Materials Sciences, Office of Basic Energy Sciences, U.S. Department of Energy.

APPENDIX

WEAR TEST MACHINE OPERATION PROCEDURE

I. Specimen Preparation - See Figure 10

1. Grind wear surface to specific roughness.
2. Ultasonically clean in acetone and dry.
3. Measure dimensions
   a. Length
   b. Diameter
   c. Depth of thermocouple hole
4. Measure weight

II. Disk Preparation

1. Grind surface to specific roughness.
2. Ultasonically clean in acetone and dry.
3. Measure thickness
4. Measure weight

III. Instrumentation Hookup - See Figures 8 and 9

1. Turn power on to oscilloscope, chart-recorder, Q-Plug unit-power supply, and thermocouple indicator.
2. Connect Strain-gage plug into Q-Plug unit.
3. Balance Q-Plug by following the Tektronix Q-Plug Unit Operation Manual.
4. Connect thermocouple to thermocouple indicator.

IV. Apparatus Set-Up - See Figure 4

1. Mount specimen in sample-holder with grinding direction parallel to direction of motion of the disk at contact position.
2. Adjust sample holder in load arm so that load arm is horizontal.

3. With applied weight off and counterbalance weight on the load arm, adjust counterbalance weight so that load arm is balanced through the pivot-point.
4. Mount desired applied weight, making sure weight is centered on weight holder pin.
5. Position shield around wear disk.
6. Connect dash-pot to load arm.
7. Place thermocouple through sample holder and into specimen.

V. Calibration of Strain-Gage

1. Zero force input on chart recorder, using vertical position switch on Q-Plug Unit. Be sure that strain-gage assembly is in neutral position.
2. Apply dead weight through pulley assembly using cable. Attach the cable to the set-screw on load arm and thread through pulley, then down through hole in the table top and hang weight.
3. Record force on chart recorder.

VI. Start-up of Test

1. Start chart recorder at desired chart speed.
2. Lift specimen (load arm) off of wear disk.
3. Turn on motor control unit and set desired speed, using tach-generator voltmeter.
4. Lower specimen (load arm) onto moving wear disk and let go of load arm.
5. Start taking needed test data.

6. Adjust dash-pot to eliminate excessive load arm lateral vibration.

VII. Shut-down of test

1. Lift specimen (load arm) off of moving wear disk.
2. Turn off motor control unit.
3. Remove specimen.
4. Clean-up.

REFERENCES

1. M. J. Neale (editor), "Tribology Handbook," Halsted Press, John Wiley and sons, Inc., New York, N.Y., 1973, Section A7.
2. F. P. Bowden and D. Tabor, "The Friction and Lubrication of Solids, Part I and II," Clarendon Press, Oxford, 1964.
3. "Application of Advanced Materials and Fabrication Technology to Let-Down Valves for Coal Liquefaction Systems," Electric Power Research Institute report #AF-304, January 1977, pp. 20-33.
4. "Wear Resistance and Impact Strength, Key Factors in Selecting Dies," Metal Progress, February 1974, pp. 67-69.
5. S. G. Bailey and C. M. Perrott, "Wear Processes Exhibited by WC-Co. in "Rotary Cutter Mining," Wear, Vol. 29, 1974, pp. 117-128.
6. J. H. Westbrook, R. K. DiCerbo and A. J. Peat, "The Nickel-Titanium-Silicon System," General Electric Technical Information Series No. 58-RL-2117, November 1958.
7. T. S. Eyre and R. K. Walker, "Wear of Sintered Metals," Powder Metallurgy, No. 1, 1976, pp. 22-30.
8. K. Gopinath, G. V. N. Rayuda and R. G. Narayanamurthi, "Friction and Wear of Sintered Iron," Wear, Vol. 42, 1977, pp. 245-250.
9. C. Amsallem, A. Gaucher and G. Guilhot, "The Unlubricated Friction Behavior of Sintered Iron," Wear, Vol. 23, 1973, pp. 97-112.
10. "Tribaloy Intermetallic Materials," Bulletins No. 1 & 2, Revised June 1973, DuPont "Tribaloy" Products Glasgon Site, Wilmington, Delaware, 19898.

11. M. J. Neale, op. cit., section F6.

12. E. Rabinowicz, "Friction and Wear of Materials," John Wiley and Sons, Inc., New York, N.Y., 1965, p. 125.

13. Catalog of the Wakefield Bearing Corporation, 1965, 22-29 Foundry Street, Wakefield, Massachusetts, 01881, USA.

14. J. F. Archard, "The Contact and Rubbing of Flat Surfaces," J. Applied Physics, Vol. 24, 1953, pp. 981-988.

15. Rabinowicz, op. cit., p.168.

16. M. J. Neale, op. cit., Section F6.

17. J. Klein, (M.S. Thesis), "A Preliminary Investigation of Liquid Phase Sintering in Ferrous Systems," MMRD-LBL, LBL No. 3549, Dept. of Mech. Eng., U.C. Berkeley, 1975.

18. A. Begelinger and A. W. J. deGee, "Synopsis of the Results from an International Cooperative Wear Program," Lubrication Engineering, February 1970, pp. 56-63.

19. T. S. Eyre and R. K. Walker, op. cit., pp. 22-30.

20. "Tribaloy Intermetallic Metals," Bulletin No. 2.

21. "Powder Metallurgy Design Guidebook," Metal Powder Industries Federation, 1974, P.O. Box 2054, Princeton, New Jersey, 08540, USA, pp. 11-14.

22. J. M. Wheatley and G. C. Smith, "The Fatigue Strength of Sintered Iron Compacts," Powder Metallurgy, No. 12, 1963, pp. 141-158.

23. J. T. Barnby, D. C. Ghosh and K. Dinsdale, "The Fracture-Resistance of a Range of Sintered Steels," Powder Metallurgy, Vol. 16. No. 31, 1973, pp. 55-71.

24. K. Gopinath, et. al., pp. 245-250.

25. C. Amsallem, et. al., pp. 97-112.

26. "Tribaloy Intermetallic Materials," Bulletin No. 2.

27. T. S. Eyre and R. K. Walker, op. cit., p. 22.

28. Ibid.

29. C. Amsallem, et. al., pp. 97-112.

TABLE I

Tribaloy 400

Elemental composition - Wt. %				Laves Phase
Co	Mo	Si	Cr	Vol. %
62	28	2	8	50

The Laves phase is present as a close-packed hexagonal compound of cobalt, molybdenum, and silicon.

Melting temperature 2250-2900°F (1230-1590°C)

Density 0.325 lb/in^3 (9.0 x 10^3 kg m^3)

Ultimate tensile strength

At 70 F (21°C)	100,000 psi (690 MN/M^2)
At 1500 F (816°C)	90,000 psi (620 MN/M^2)

Hardness:

Laves phase: 1000 - 1200 VHN
Overall: Rockwell C 50 - 60

TABLE II

SINTERING PAAMETERS OF TEST SAMPLES

Material	Compaction Pressure (ksi)	Sintering Temperature (^{o}C)	Sintering Time (min)	Vacuum (mm of Hg)	Wear Test Numbers
Fe	100	1150	60	3×10^{-5}	1, 2, 3, 5
Fe + 20 w/o G'	100	1250	60	4×10^{-6}	----------
Fe + 20 w/o G'	100	1150	15	6×10^{-6}	12, 13, 14, 20
Fe + 20 w/o G'	100	1150	30	6×10^{-6}	7, 8, 9
Fe + 20 w/o G'	100	1150	60	5×10^{-6}	10, 11, 19
Fe + 20 w/o G'	100	1000	15	5×10^{-6}	---------
Fe + 20 w/o G'	100	1000	30	5×10^{-6}	24, 25, 26, 27
Fe + 20 w/o G'	100	1000	60	4×10^{-6}	---------
Fe + 20 w/o G'	100	Arc-melted		--------	21, 22, 23
Fe + 11 w/o Commercial Additive	100	1150	60	3×10^{-6}	4, 6
Fe + 22 w/o Commercial Additive	100	1150	60	4×10^{-6}	15, 16, 17, 18

TABLE III

DENSITY AND GENERAL HARDNESS OF SAMPLES

Sinter (temp. ^{o}C , time min)	Density (gm/cm^3)	% Theoretical Density	Hardness Rockwell	Wear Test Numbers
Fe	7.04	89.4	R_B55	1, 2, 3, 5
Fe + 20 w/o G' (1250, 60)	----	----	R_B70	---------
Fe + 20 w/o G' (1150, 15)	5.71	78.2	R_B70	12, 13, 14, 20
Fe + 20 w/o G' (1150, 30)	5.91	80.8	R_B74	7, 8, 9
Fe + 20 w/o G' (1150, 60)	6.27	85.8	R_B74	10, 11, 19
Fe + 20 w/o G' (1000, 15)	6.85	93.7		---------
Fe + 20 w/o G' (1000, 30)	6.78	93.0	R_B55	24, 25, 26, 27
Fe + 20 w/o G' (1000, 60)	6.77	92.6		---------
Fe + 20 w/o G' (Arc-melted)	7.31	100	R_C37	21, 22, 23
Fe + 11 w/o Commercial	7.24	90.8	R_B20	4, 6
Fe + 22 w/o Commercial	6.95	85.8	R_B57	15, 16, 17, 18

TABLE IV

SUMMARY OF WEAR TESTS

Test No.	Material	Sintering Time, Temp. °C, Min.	Normal Force $kgf/m^2 \times 10^{-4}$	Sliding Speed (m/sec)	Test Time (hr)	Wear Rate $gm/m \times 10^6$	Coeff. of Friction	Temp. of Sample (°C)	Comments
1	Fe	1150, 60	19.8	2	1	28.5	0.518	100	Smearing of end
2	Fe	1150, 60	19.8	2	2	23.0	0.525	120	Smearing of end
3	Fe	1150, 60	19.8	2	2	6.34	0.494	115	Smearing of end
4	Fe + 11 w/o T-400	1150, 60	19.8	2	0.28	368.4	-----	200	Wore excessively fast
5	Fe	1150, 60	19.8	2	1	15.8	0.542	120	Smearing of end
6	Fe + 11 w/o T-400	1150, 60	5.40	2	2	4.59	0.541	57	
7	Fe + 20 w/o G'	1150, 30	19.8	2	2	2.00	0.539	110	More vibration
8	Fe + 20 w/o G'	1150, 30	19.8	2	2	5.63	0.478	128	
9	Fe + 20 w/o G'	1150, 30	19.8	2	2	1.53	0.474	104	
10	Fe + 20 w/o G'	1150, 60	19.8	2	2	45.7	0.459	230	Some chattering
11	Fe + 20 w/o G'	1150, 60	19.8	2	2	40.1	0.498	160	
12	Fe + 20 w/o G'	1150, 15	19.8	2	1	64.6	0.478	220	Disk machined incorrectly
13	Fe + 20 w/o G'	1150, 15	19.8	2	2	1.58	0.485	98	
14	Fe + 20 w/o G'	1150, 15	19.8	2	2	3.09	0.486	100	
15	Fe + 22 w/o T-400	1150, 60	19.8	2	2	14.9	0.509	120	
16	Fe + 22 w/o T-400	1150, 60	19.8	2	2	10.1	0.510	110	
17	Fe + 22 w/o T-400	1150, 60	19.8	2	0.50	204.5	-----	200	Wore excessvely fast
18	Fe + 22 w/o T-400	1150, 60	19.8	2	2	11.7	0.494	130	
19	Fe + 20 w/o G'	1150, 60	19.8	2	2	36.5	0.447	185	
20	Fe + 20 w/o G'	1150, 15	19.8	2	2	2.51	0.463	100	

TABLE IV (Continued)

SUMMARY OF WEAR TESTS

Test No.	Material	Sintering Time, Temp. °C, Min.	Normal Force $kgf/m^2 \times 10^{-4}$	Sliding Speed (m/sec)	Test Time (hr)	Wear Rate $gm/m \times 10^6$	Coeff. of Friction	Temp. of Sample (°C)	Comments
21	Fe + 20 w/o G'	Arc-melted	19.8	2	1	122.0	0.534	200	
22	Fe + 20 w/o G'	Arc-melted	19.8	2	1	81.2	0.531	240	
23	Fe + 20 w/o G'	Arc-melted	19.8	2	1	116.0	0.526	230	
24	Fe + 20 w/o G'	1000, 30	19.8	2	2	3.25	0.510	100	
25	Fe + 20 w/o G'	1000, 30	19.8	2	0.70	190.3	-----	220	Incorrect placement of sample
26	Fe + 20 w/o G'	1000, 30	19.8	2	2	1.93	0.526	110	
27	Fe + 20 w/o G'	1000, 30	19.8	2	2	3.64	0.536	110	

FIGURE CAPTIONS

Figure 1. Simplified picture of adhesive wear and a plot of the three degrees of adhesive wear. (M. J. Neale[1]).

Figure 2. A simplified picture of abrasive wear, and the relation between abrasive wear resistance and material hardness. (M. J. Neale[1]).

Figure 3. Pin and disk wear surface.

Figure 4. Assembly drawing of test section: (1) sample holder; (2) Strain gage assembly; (3) Load arm; (4) Gimbal assembly; (5) Counterbalance weight; (6) Applied weight holder; (7) Wear Disk; (8) Adjustable air damper (dash-pot).

Figure 5. Friction and wear test machine with speed control unit in foreground.

Figure 6. Front view of test section of the machine, with applied weight being held.

Figure 7. Rear view of test section of the machine.

Figure 8. Friction and wear test machine with instrumentation.

Figure 9. Instrumentation schematic.

Figure 10. Wear pin dimensions.

Figure 11. Green compact of Fe + 20 w/o G'. Shows distribution of darker G' particles with the lighter iron particles.

Figure 12. Fe + 20 w/o G', sintered at 1000°C and 1150°C for 30 minutes. EDAX x-ray profile analysis of the three phases present.

Figure 13. Fe + 20 w/o G', sintered at 1000°C for: a) 15 minutes, b) 30 minutes, and c) 6 minutes.

Figure 14. Fe + 20 w/o G', sintered at 1150°C for: a) 15 minutes, b) 30 minutes, and c) 60 minutes.

Figure 15. Fe + 20 w/o G', sintered at 1250°C for one hour: a) optical picture, and b) SEM picture. EDAX profile analysis of phase present.

Figure 16. Fe + 20 w/o G', Arc-melted and homogenized: a) Optical picture, and b) SEM picture. EDAX profile of phases present.

Figure 17. Sintered density vs. sintering time for Fe + 20 w/o G'. The sintering temperatures are 1000°C and 1150°C.

Figure 18. Fe + 22 w/o commercial additive.

Figure 19. Wear rate vs. sintering time of Fe + 20 w/o G', sintered at 1150°C.

Figure 20. Coefficient of friction vs. sintering time of Fe + 20 w/o G', sintered at 1150°C.

Figure 21. a) Wear pin after a test; the pin was Fe + 20 w/o G' sintered at 1150°C for 3 minutes.
b) Wear debris from this pin.

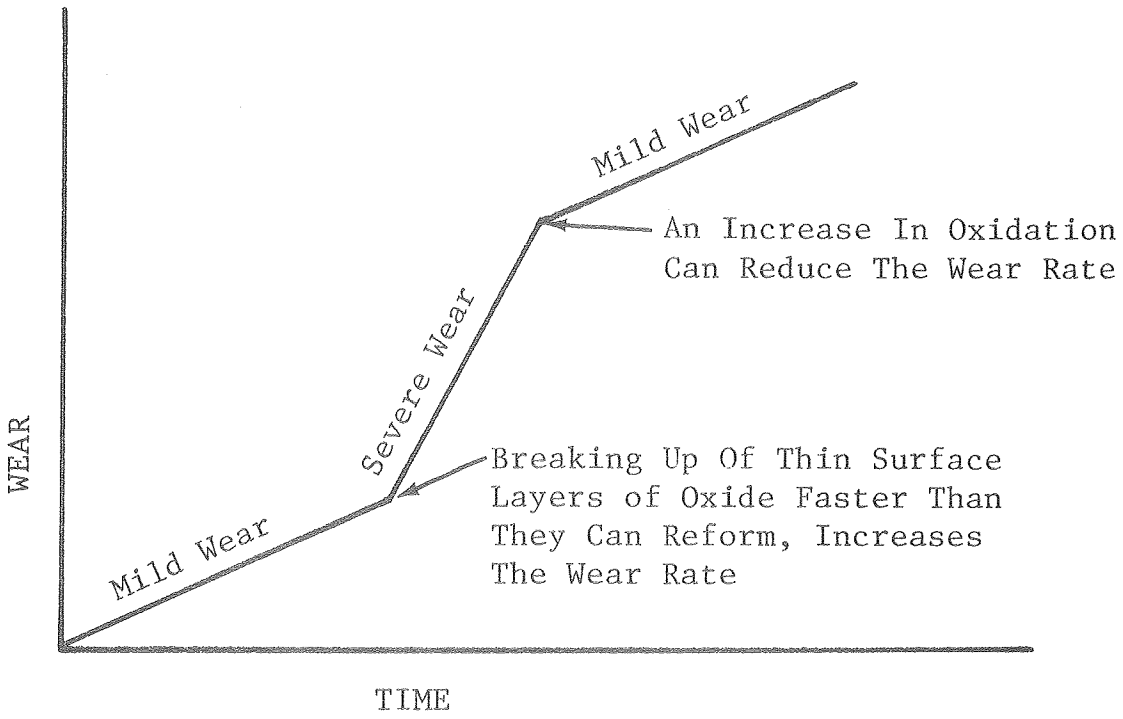

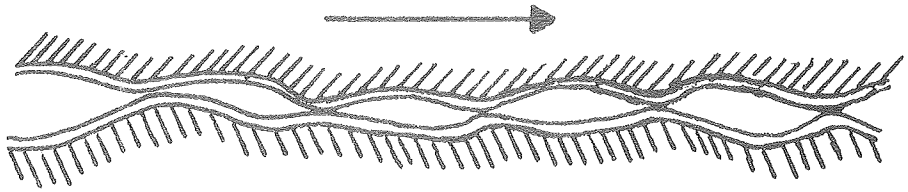

Sliding Occurring Between Surface Films

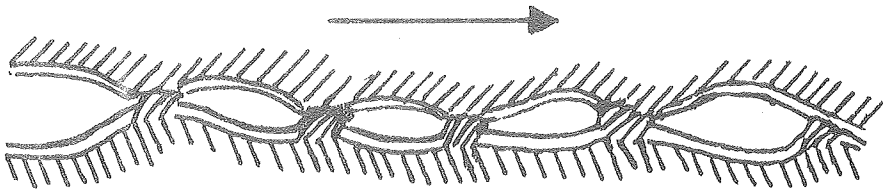

Surface Films Ruptured with Direct
Interaction Between the Materials

XBL 7711-10509

Fig. 1

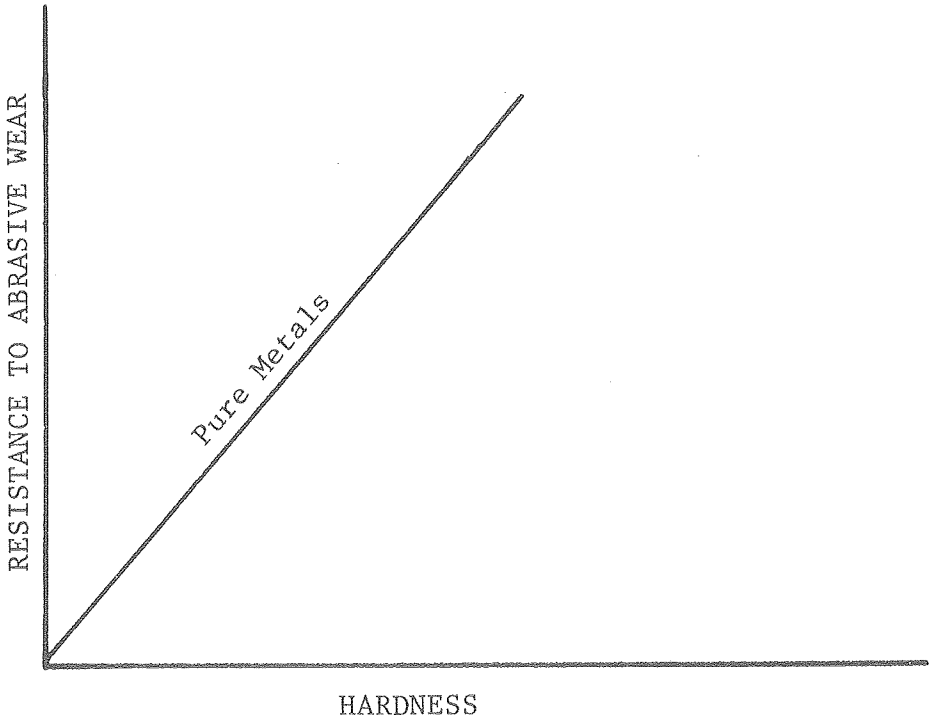

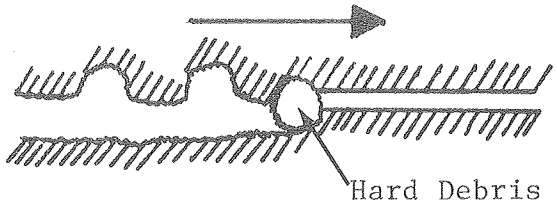

Sliding Between Two Surfaces

XBL 7711-10508

Fig. 2

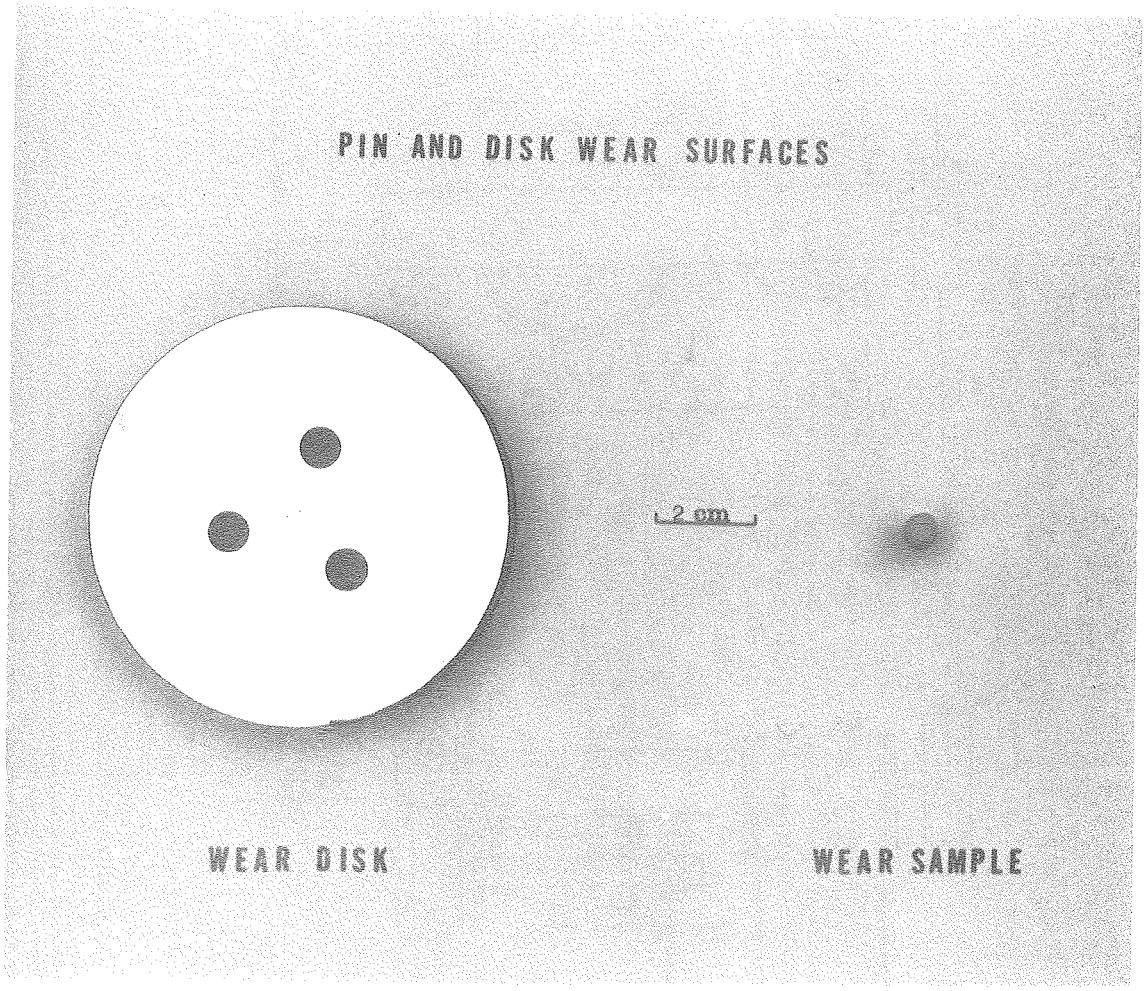

XBB 779-8897

Fig. 3

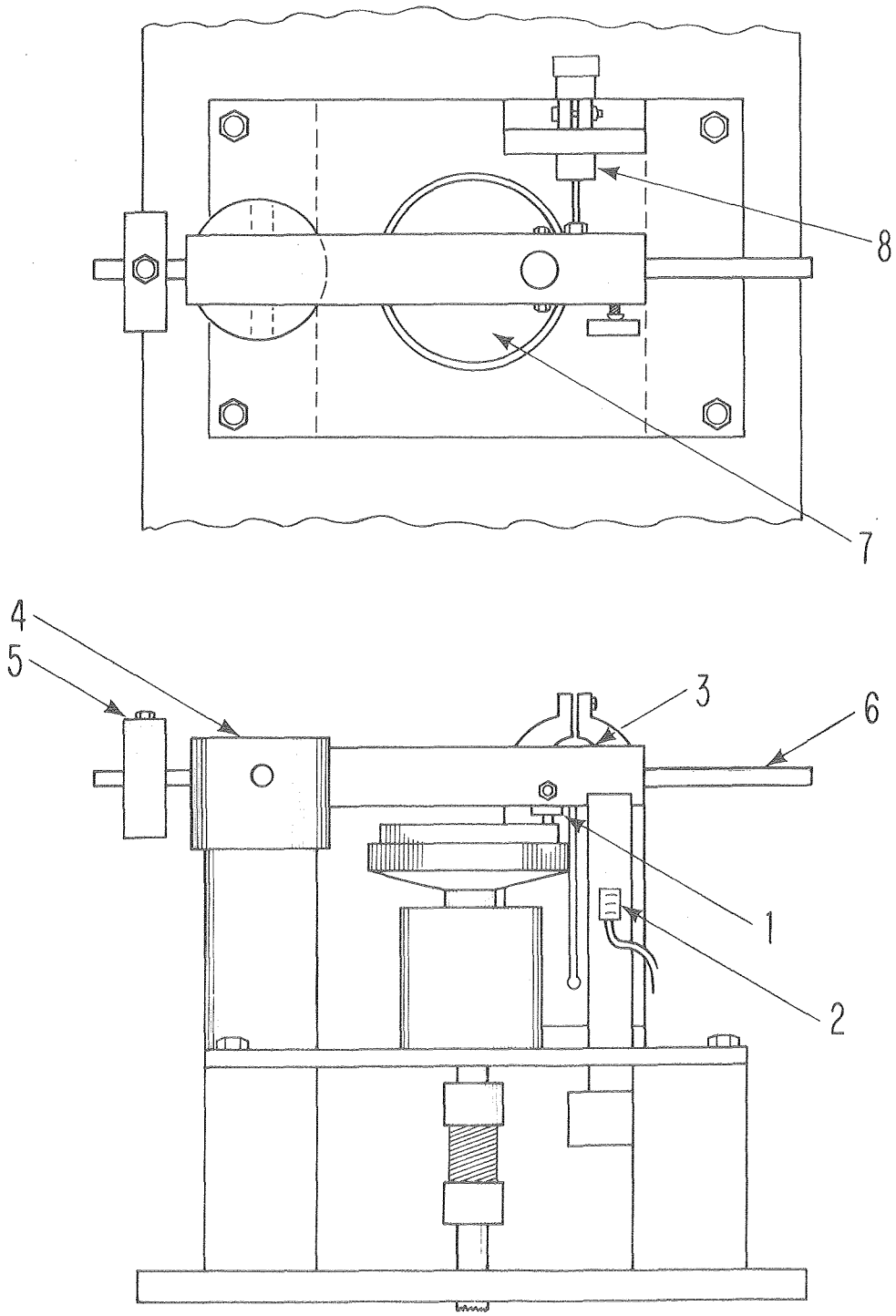

XBL7710-2129

Fig. 4

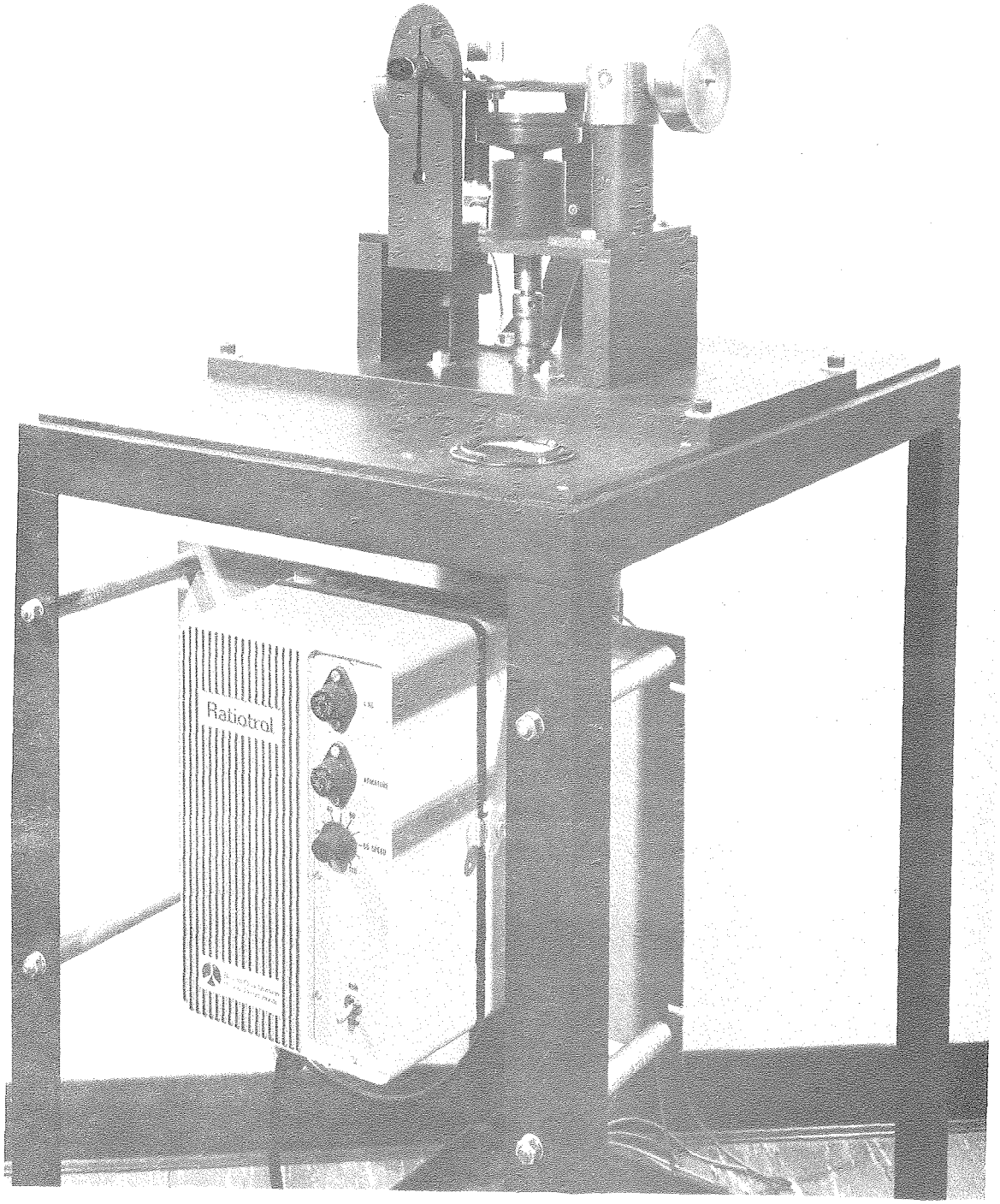

XBB 779-8894

Fig. 5

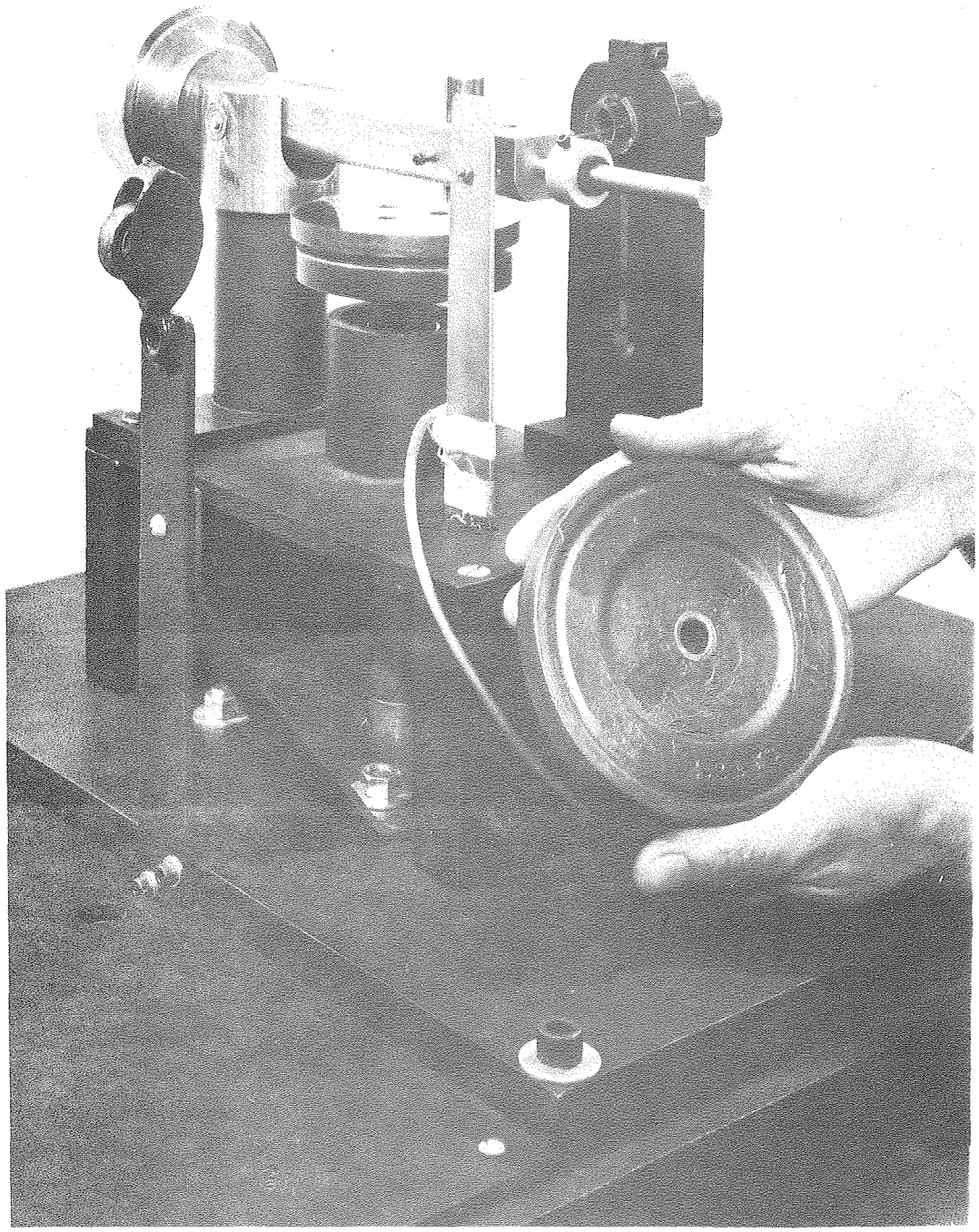

XBB 779-8896

Fig. 6

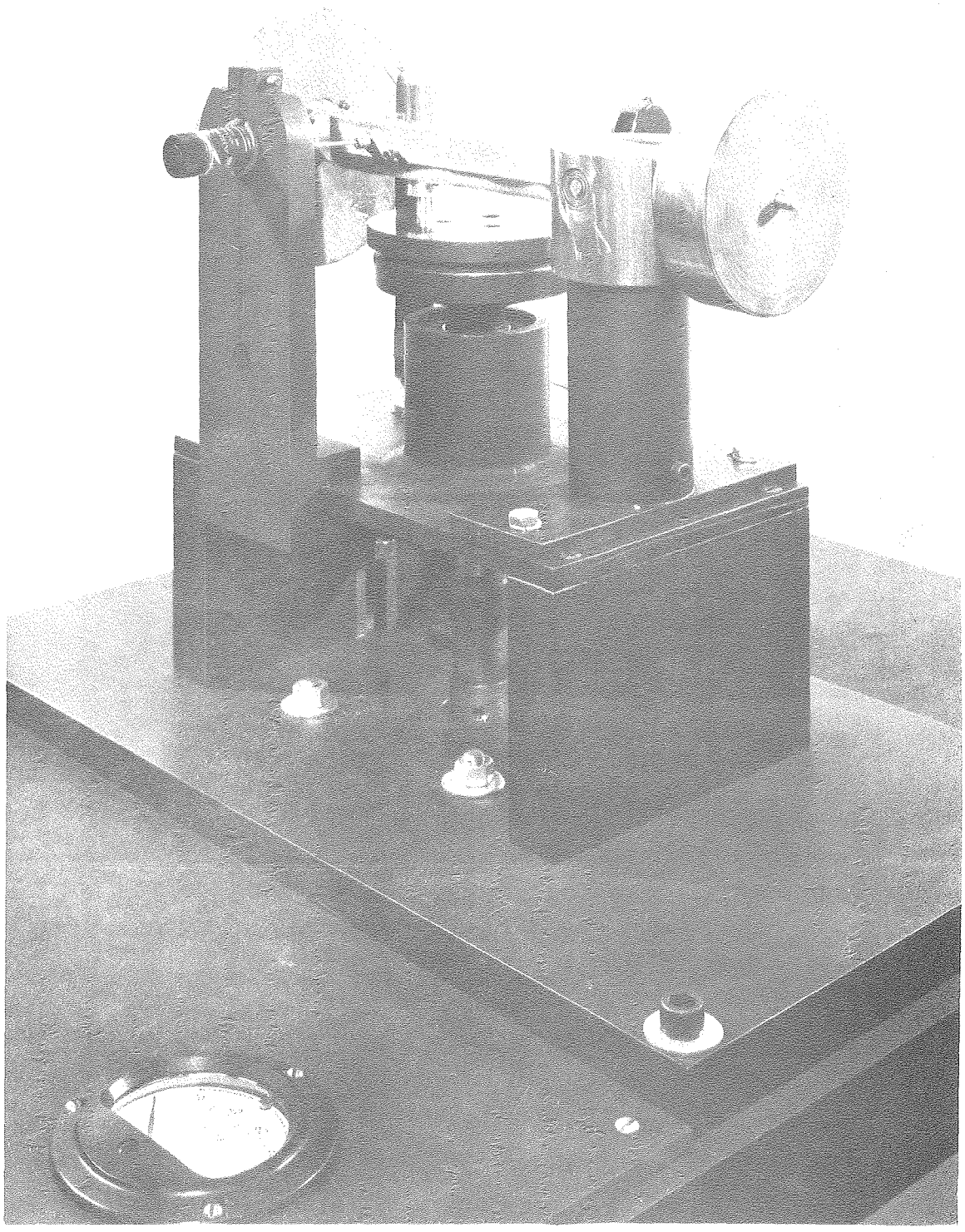

XBB 779-8892

Fig. 7

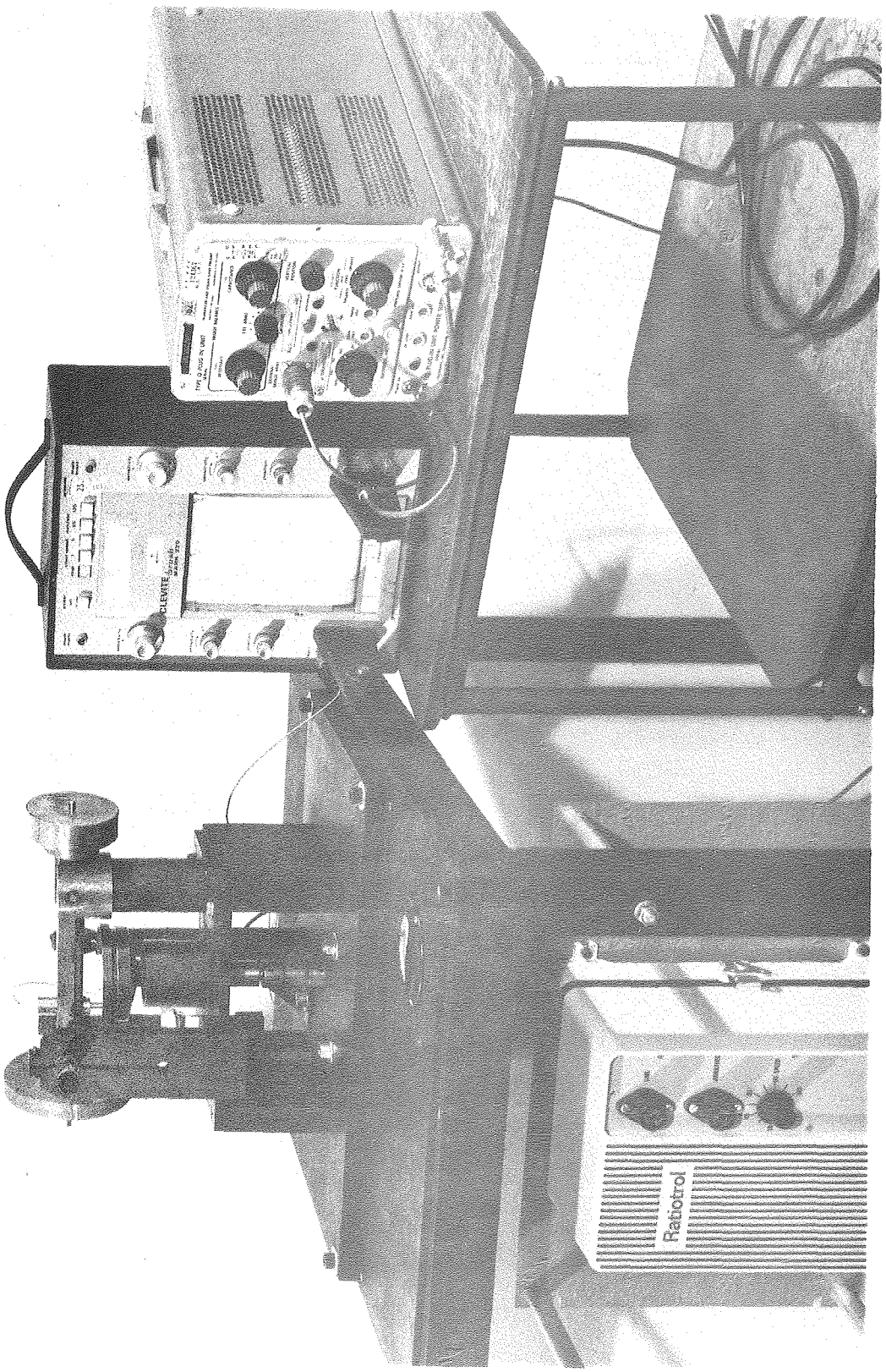

XBB 779-8895

Fig. 8

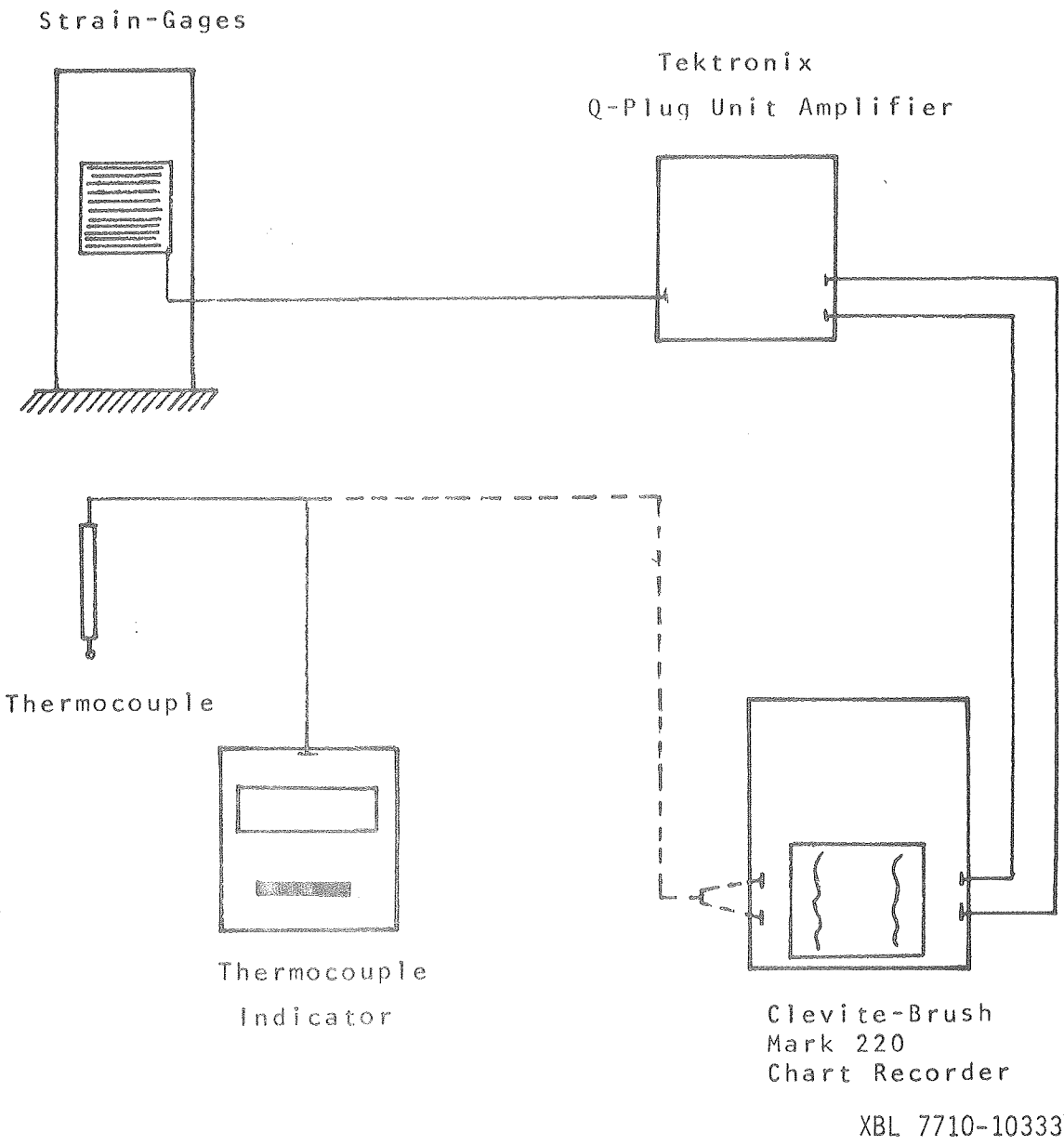
Strain-Gages
Tektronix
Q-Plug Unit Amplifier
Thermocouple
Thermocouple
Indicator
Clevite-Brush
Mark 220
Chart Recorder
XBL 7710-10333

Fig. 9

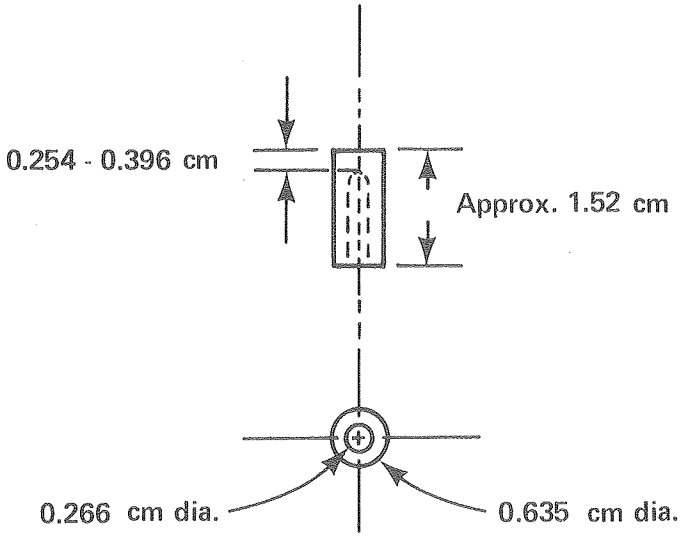

XBL 7710-2130

Fig. 10

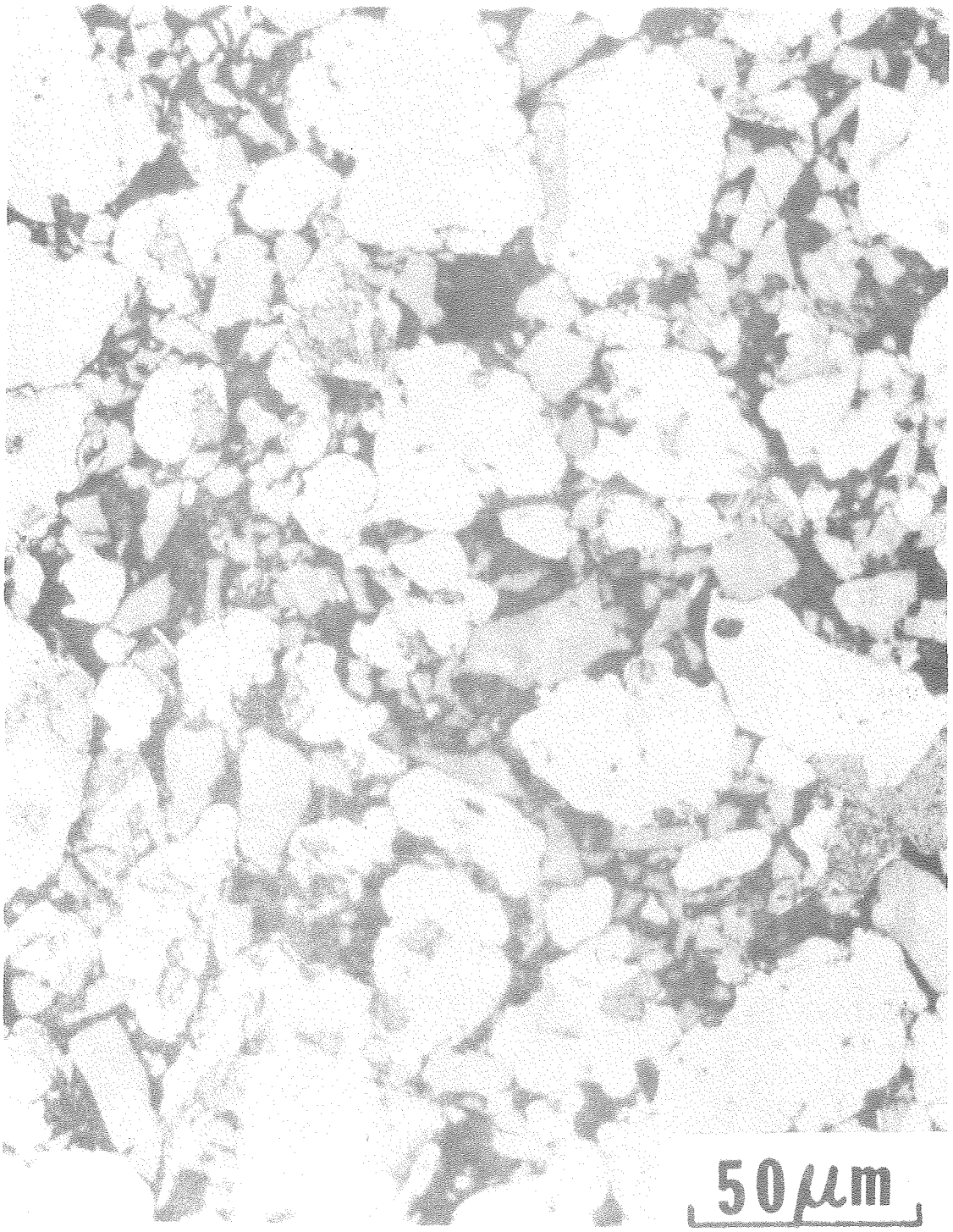

XBB 770-11353

Fig. 11

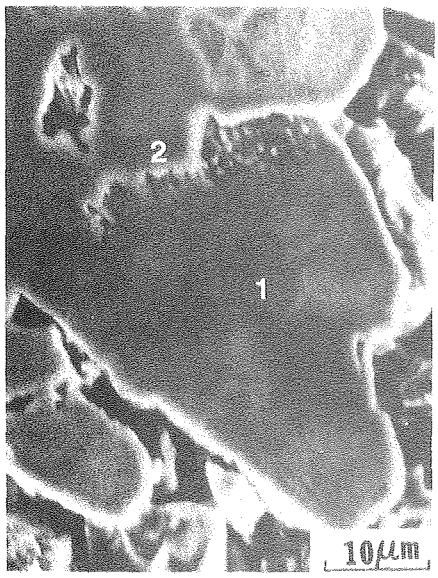

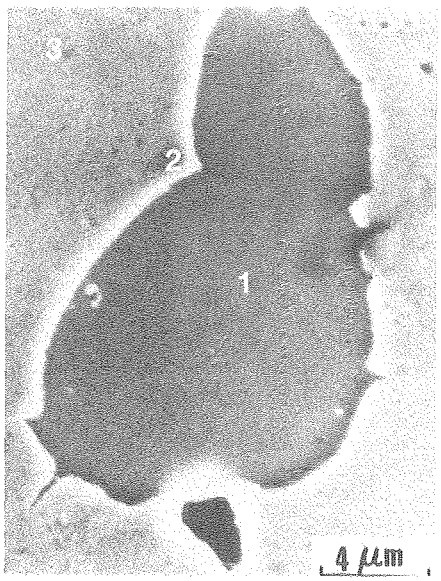

(1) G′particle
Fe 2.7wt.%
Ni 57.9
Ti 20.7
Si 18.6
VHN 440

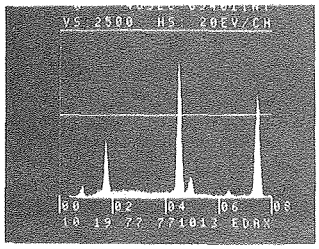

(1)G′particle
Fe 54.6 wt.%
Ni 13.5
Ti 22.5
Si 9.4
VHN 380

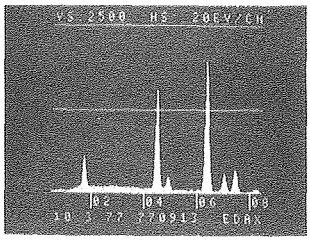

(2)Dif. zone
Fe 74.5
Ni 16.9
Ti 5.3
Si 3.3

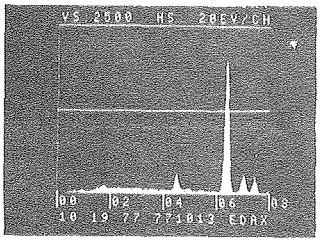

(2)Dif. zone
Fe 76.5
Ni 9.4
Ti 9.3
Si 4.8

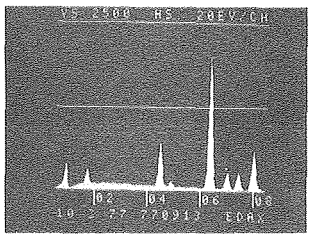

(3) Matrix
Fe 97.7
Ni 1.1
Ti 0.9
Si 0.3
VHN 94

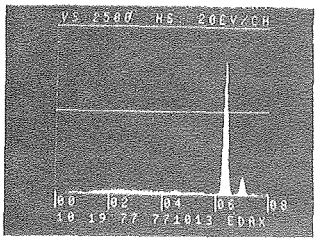

(3) Matrix
Fe 82.4
Ni 12.9
Ti 3.2
Si 1.5
VHN 300

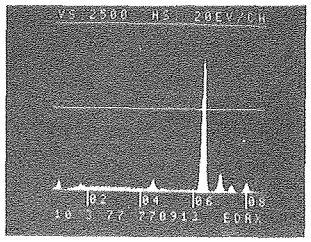

Sintered
30min. 1000 °C

Sintered
30 min. 1150 °C

XBB 770-11387

Fig. 12

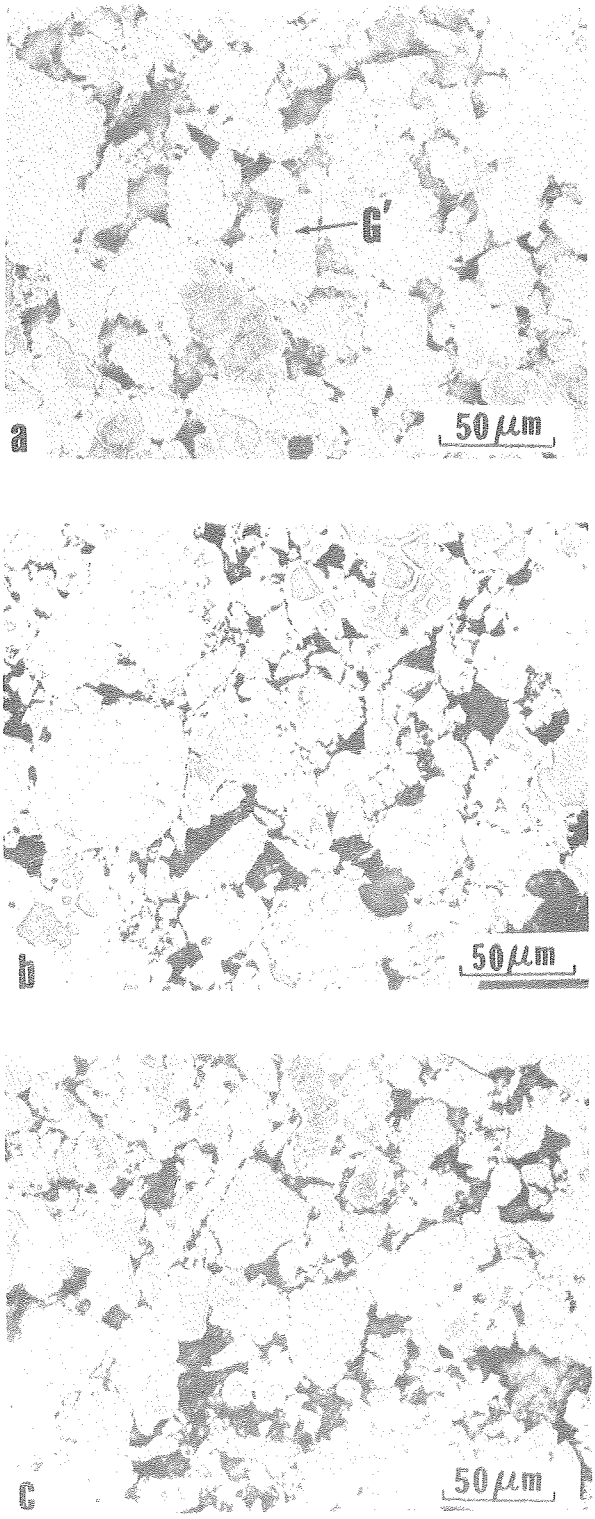

XBB 770-11351

Fig. 13

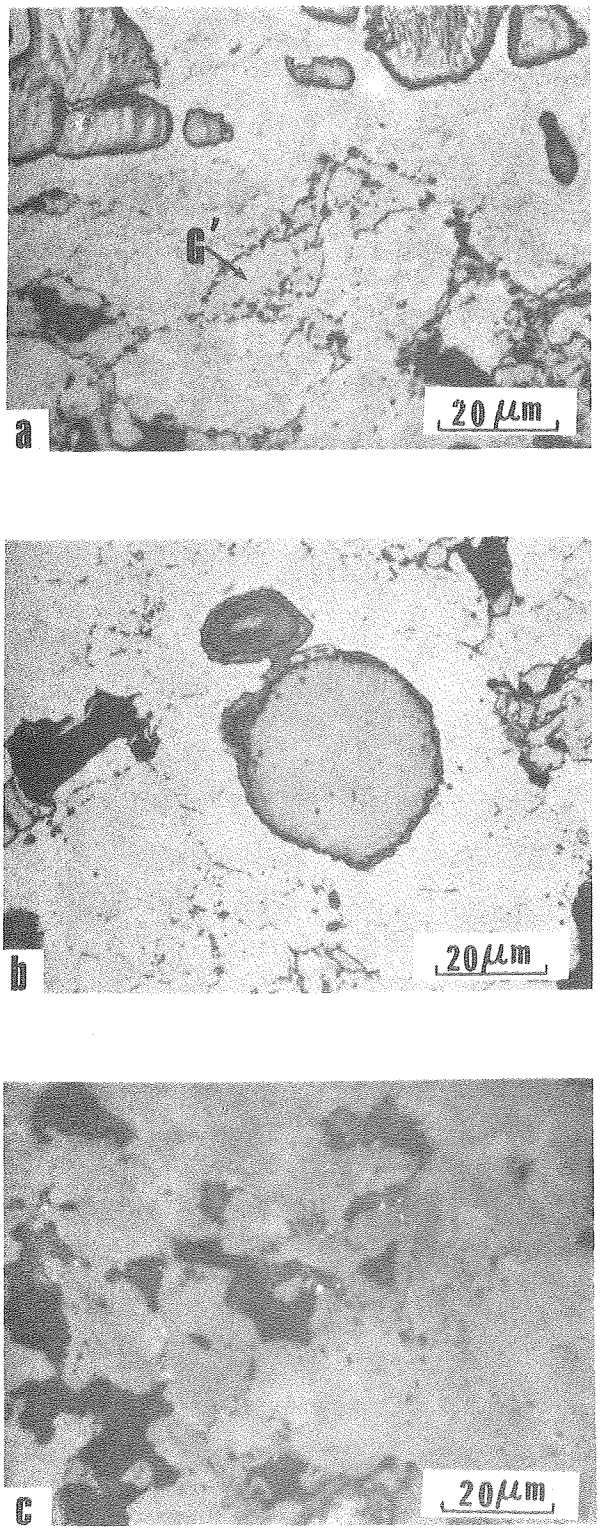

XBB 770-11350

Fig. 14

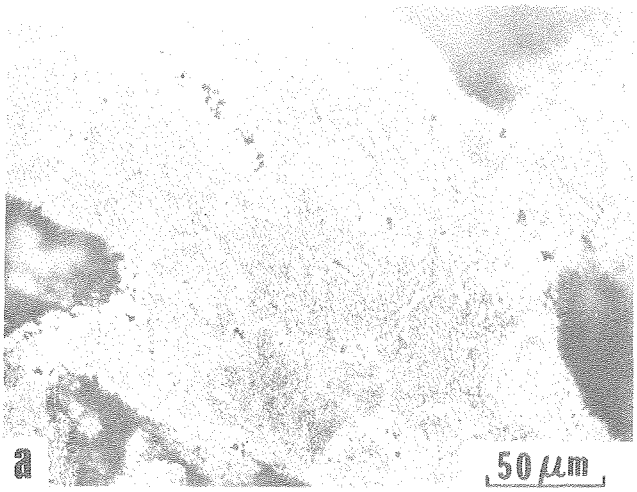

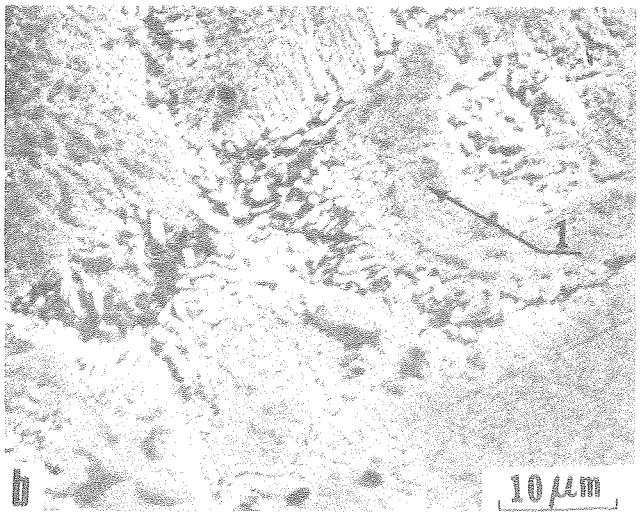

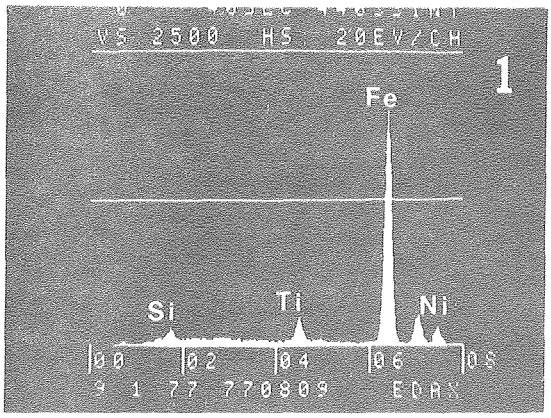

XBB 770-11354

Fig. 15

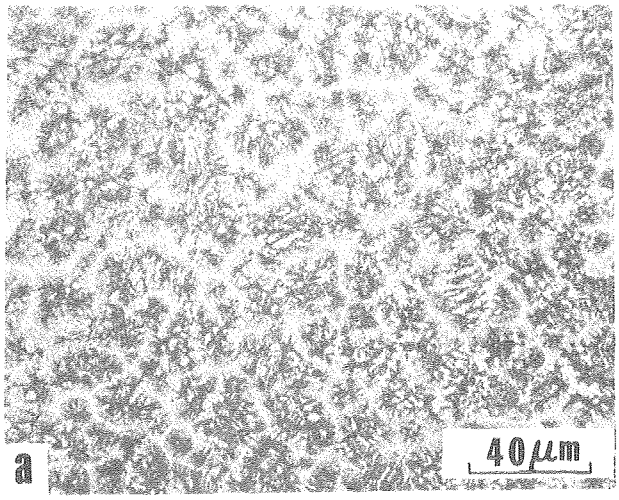

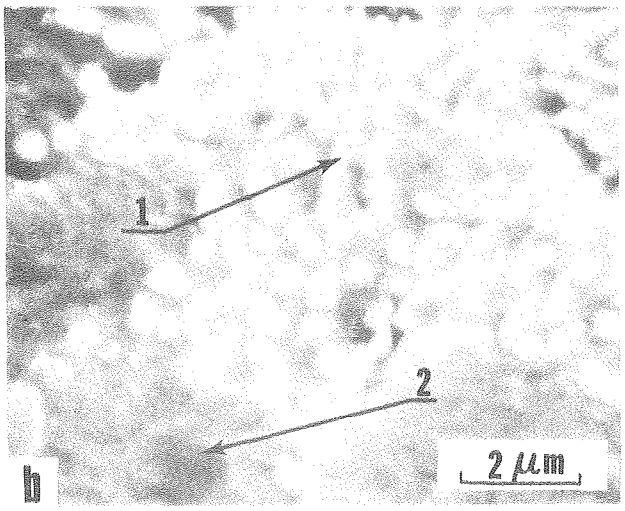

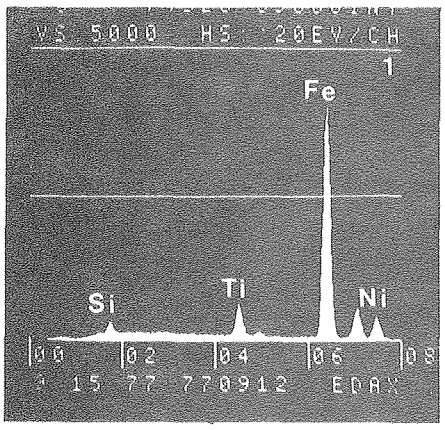

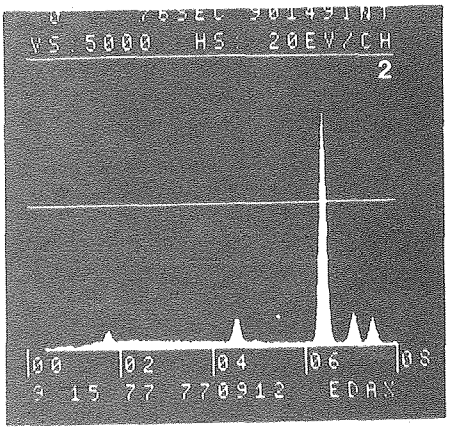

XBB 770-11352

Fig. 16

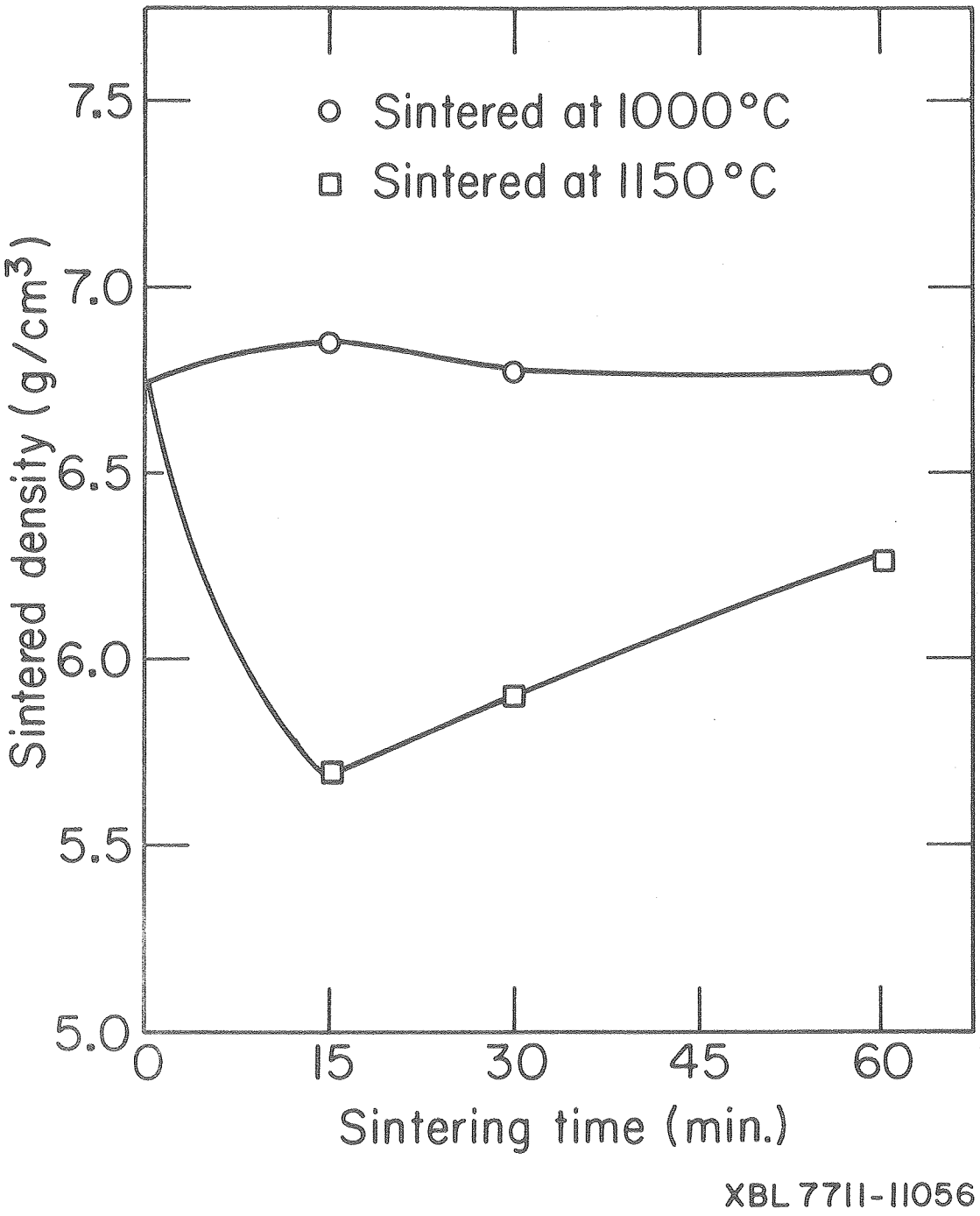
Sintered at 1000°C
Sintered at 1150°C
Sintered density (g/cm³)
7.5
7.0
6.5
6.0
5.5
5.0
0
15
30
45
60
Sintering time (min.)
XBL 7711-11056

Fig. 17

XBB 770-10877

Fig. 18

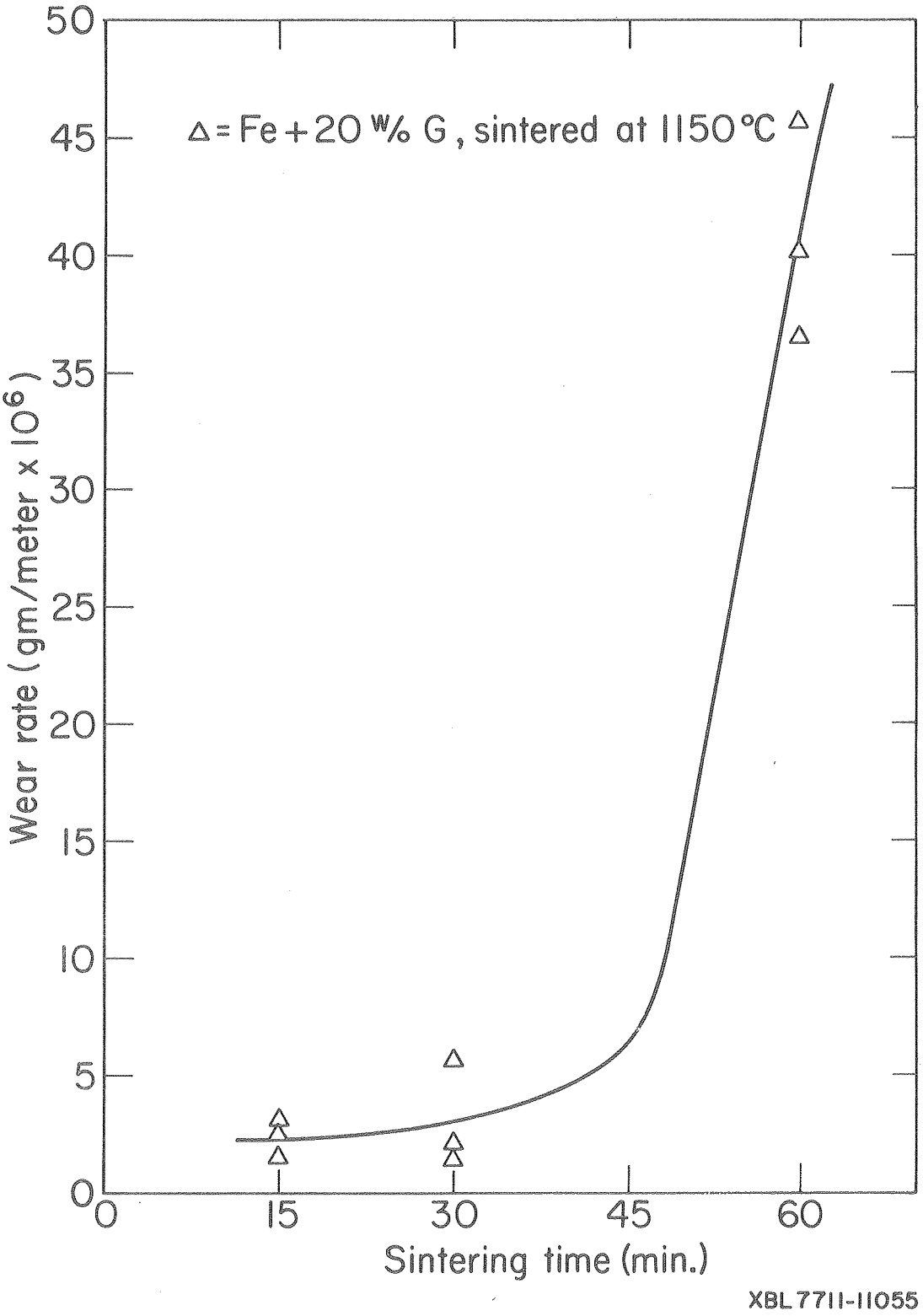
Δ = Fe + 20 w% G, sintered at 1150°C
Wear rate (gm/meter x 10⁶)
Sintering time (min.)
0
5
10
15
20
25
30
35
40
45
50
0
15
30
45
60
XBL 7711-11055

Fig. 19

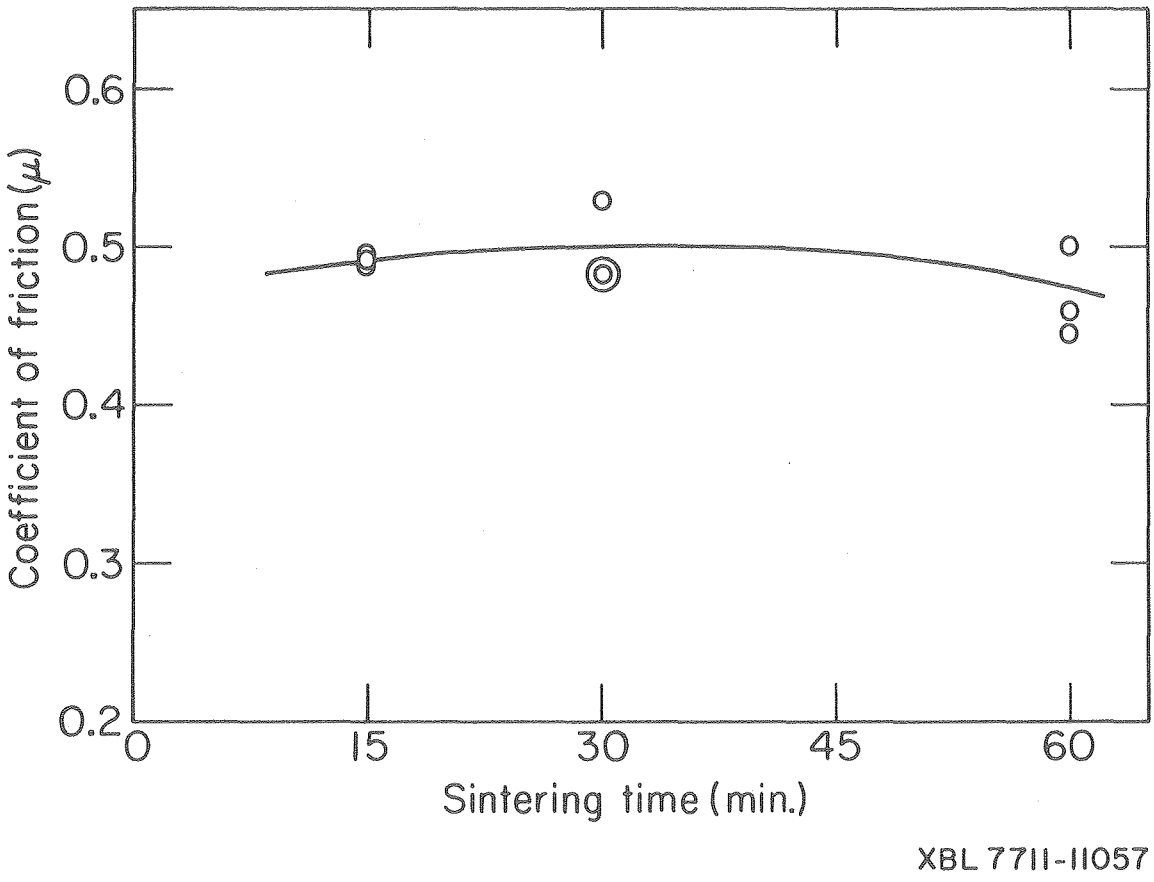
Coefficient of friction (μ)
0.6
0.5
0.4
0.3
0.2
0
15
30
45
60
Sintering time (min.)
XBL 7711-11057

Fig. 20

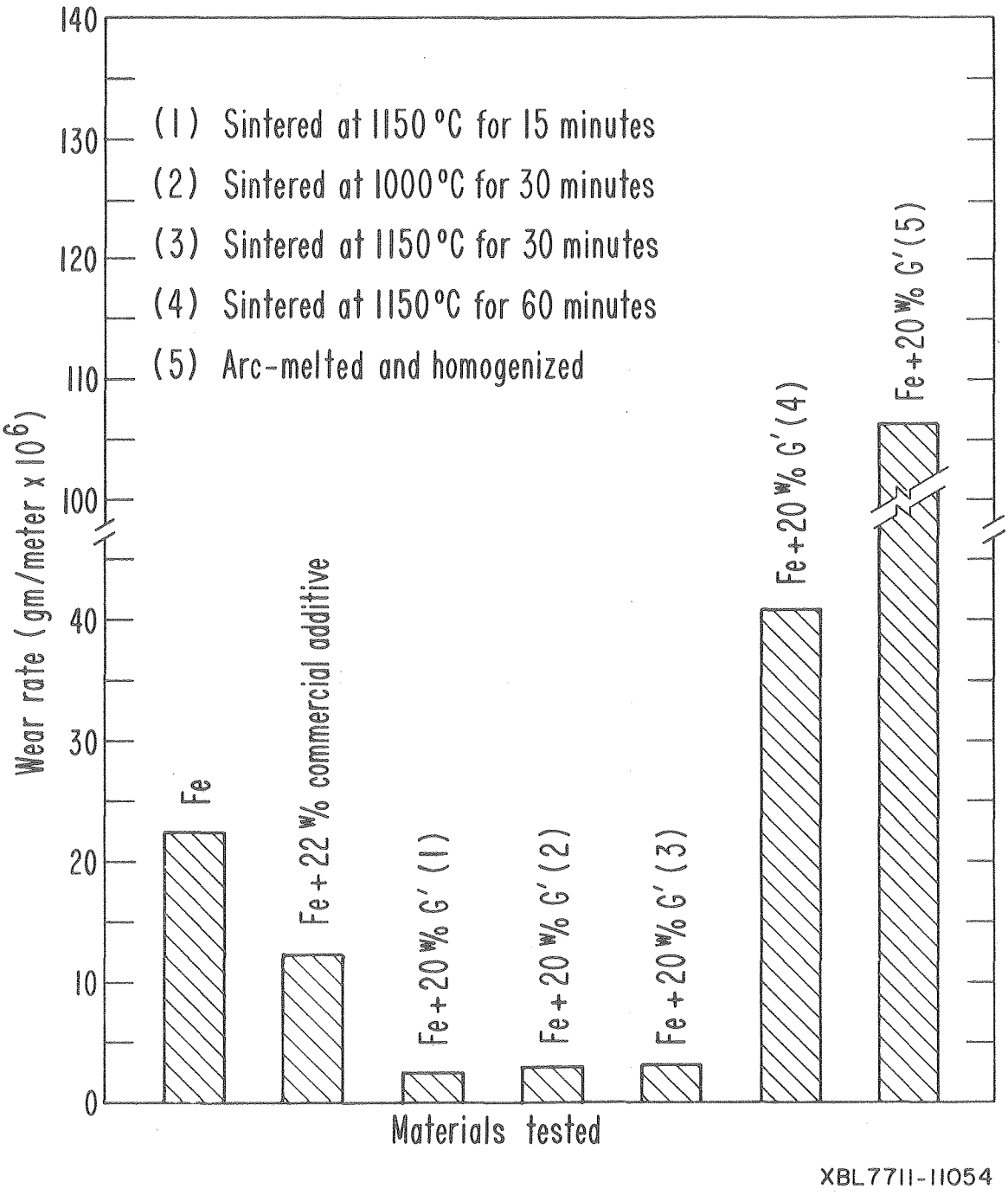
(1) Sintered at 1150 °C for 15 minutes
(2) Sintered at 1000 °C for 30 minutes
(3) Sintered at 1150 °C for 30 minutes
(4) Sintered at 1150 °C for 60 minutes
(5) Arc-melted and homogenized
Wear rate (gm/meter x 10^6)
140
130
120
110
100
40
30
20
10
0
Fe
Fe + 22 w% commercial additive
Fe + 20 w% G' (1)
Fe + 20 w% G' (2)
Fe + 20 w% G' (3)
Fe + 20 w% G' (4)
Fe + 20 w% G' (5)
Materials tested
XBL7711-11054

Fig. 21

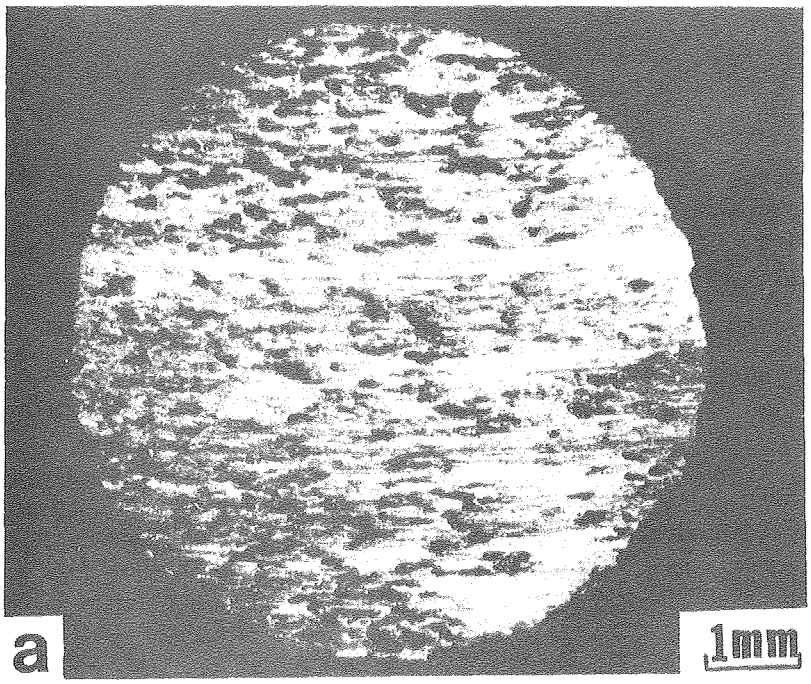
a
1mm

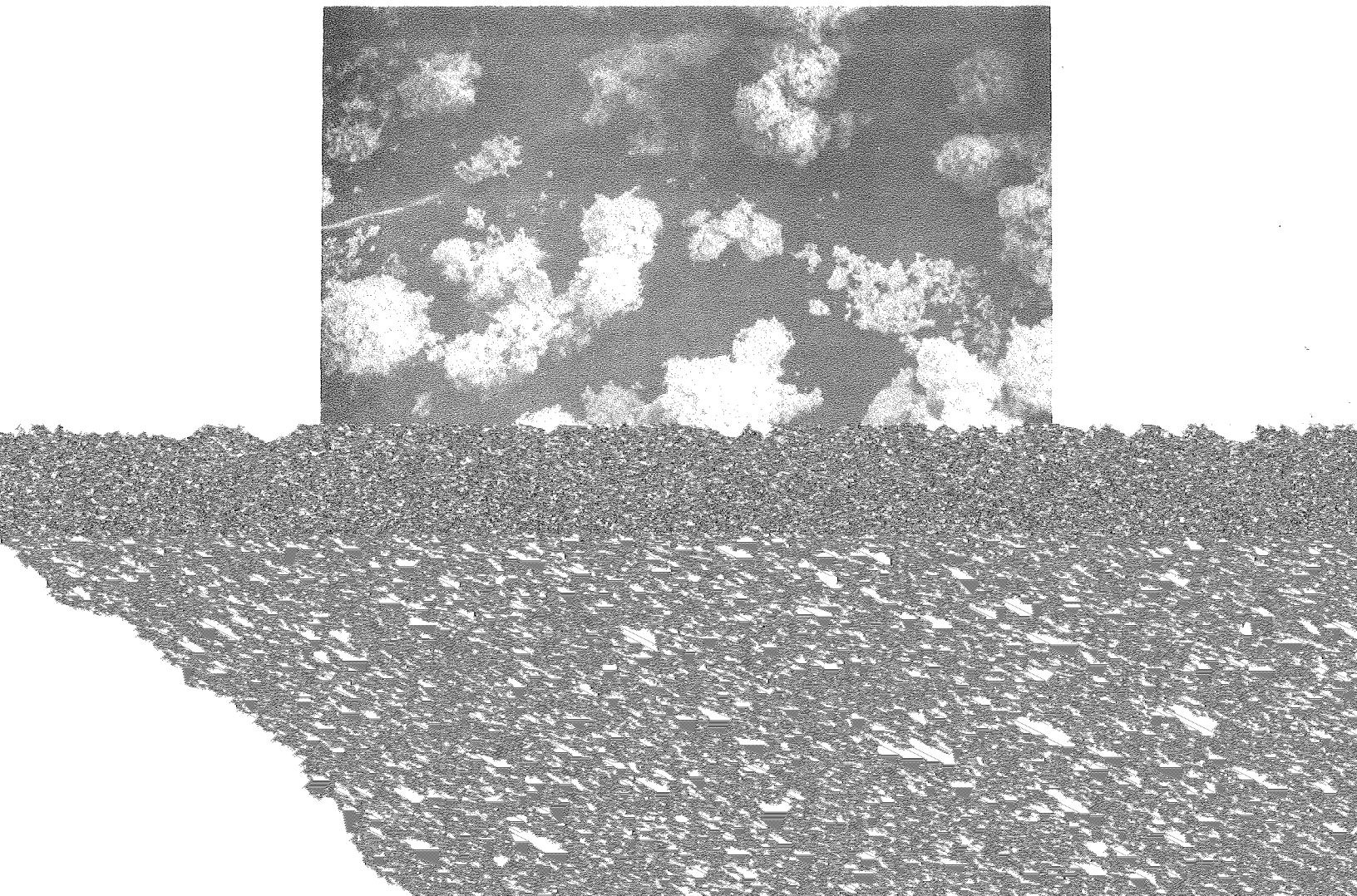

This report was done with support from the United States Energy Research and Development Administration. Any conclusions or opinions expressed in this report represent solely those of the author(s) and not necessarily those of The Regents of the University of California, the Lawrence Berkeley Laboratory or the United States Energy Research and Development Administration.

0 0 0 0 4 5 0 2 2 9 4